Study on the Flood Forecasting for Medium and Small River Watersheds Based on Multi-source Information Fusion

Ke Zhang

Yangtze Institute for Conservation and Development

College of Hydrology and Water Resources

Hohai University

Sept 22, 2023

Email: kzhang@hhu.edu.cn

Outline

1. Motivation
2. Multi-source precipitation merging
3. Remote sensing of watershed states
4. Modelling of runoff yield and concentration
5. Conclusions

1. Motivation

Classification of rivers in terms of size

- Ditches and streams： contributing area ≤ 200 km^2
- Medium and small rivers： 200 km^2 < contributing area < 3000 km^2
- Large rivers： contributing area ≥ 3000 km^2

China has more than 9900 medium and small rivers!

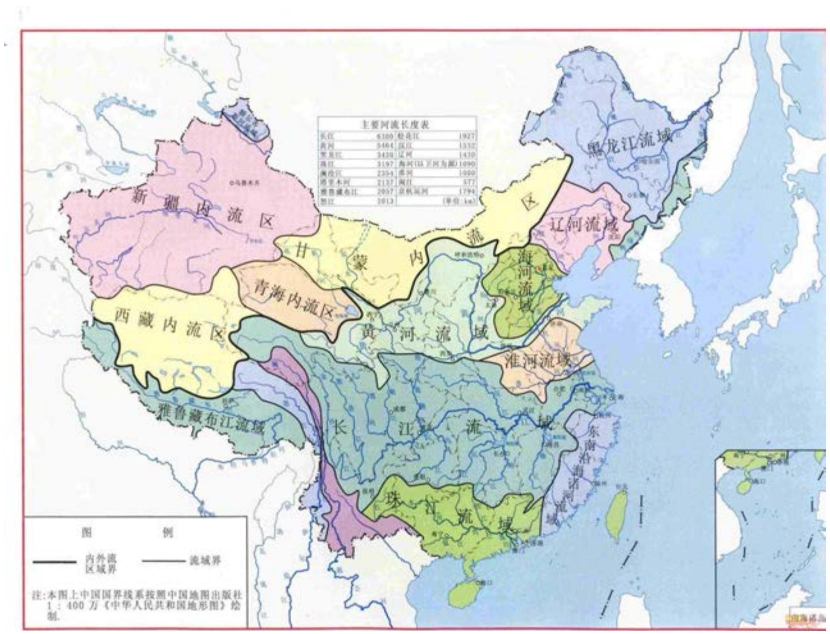

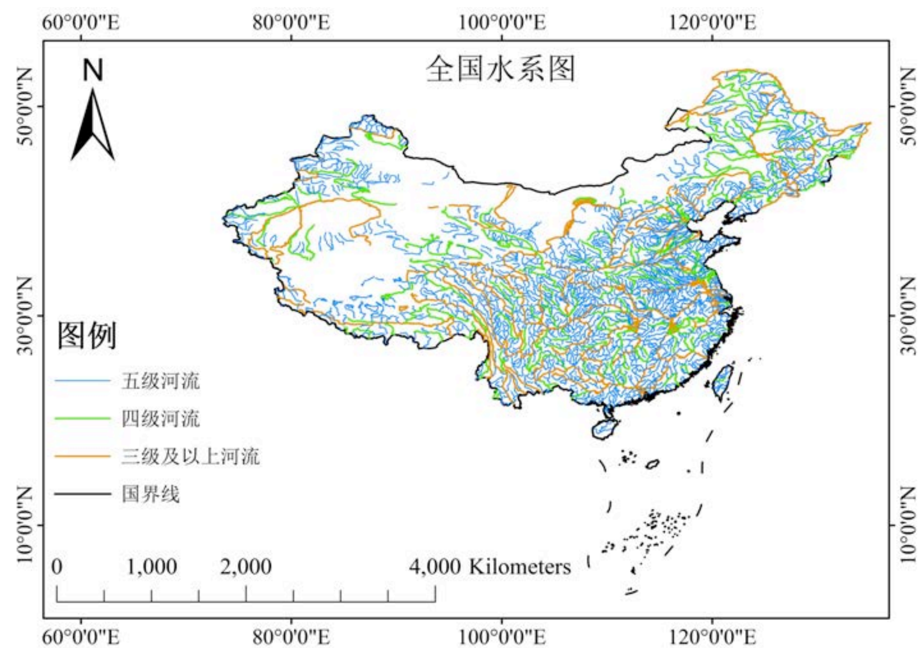

Source: China’s National Fundamental GIS Data Center

1. Motivation

Flooding and water-logging are one of the most severe natural hazards in China:

- ➢ Since 2010, annual property loss is about 200 billion RMB
- ➢ In 2010, 2016 and 2020, 30 provinces suffered floods and water-logging and 100+ rivers experienced historical floods, causing a direct economic loss of 350+ billion RMB

Percentages of different natural hazards in China (China Hazards Report)

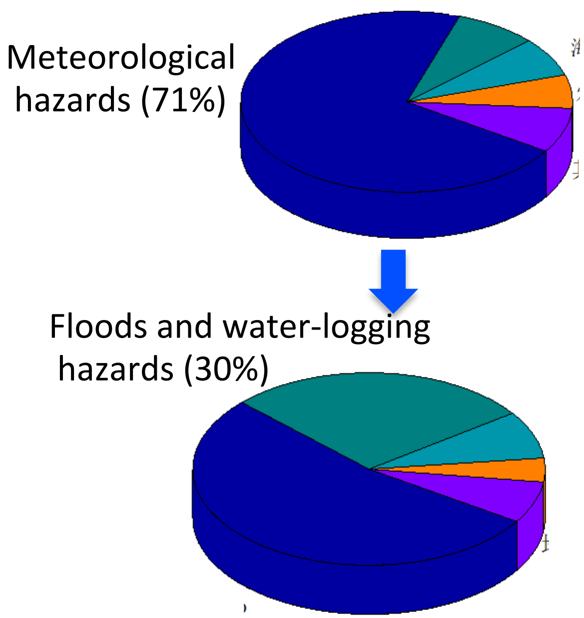

Direct economic losses caused by floods and water-logging from 2005-2018 (China Water and Drought Disasters Report)

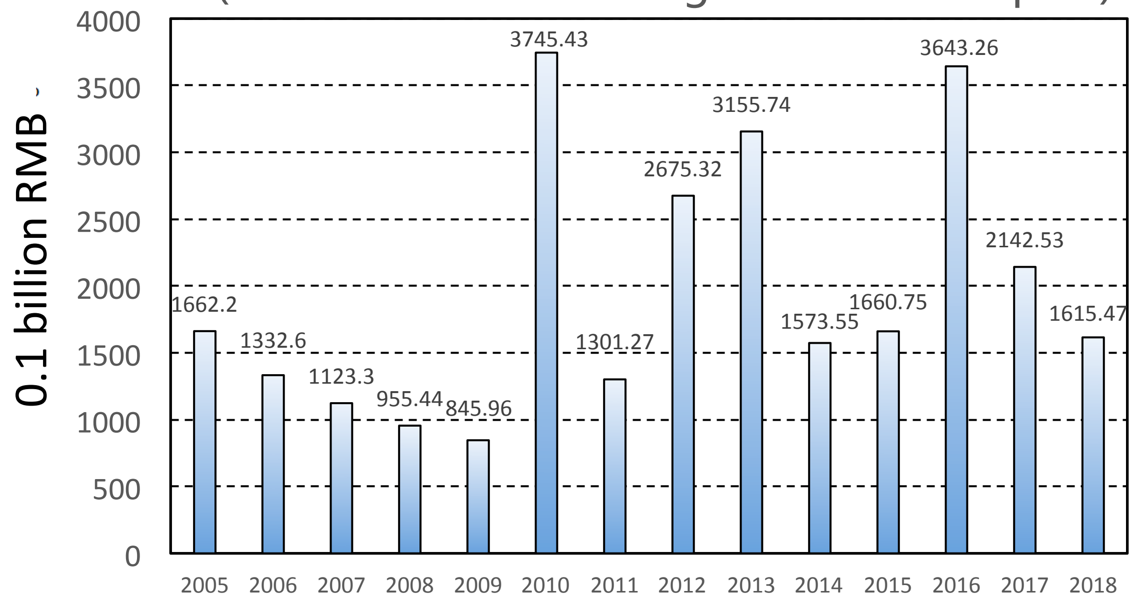

1. Motivation

- Flooding and water-logging hazards frequently occur in medium and small rivers of China
- Caused a large number of losses in lives and properties
- Becomes the major part of water-hazards losses in China

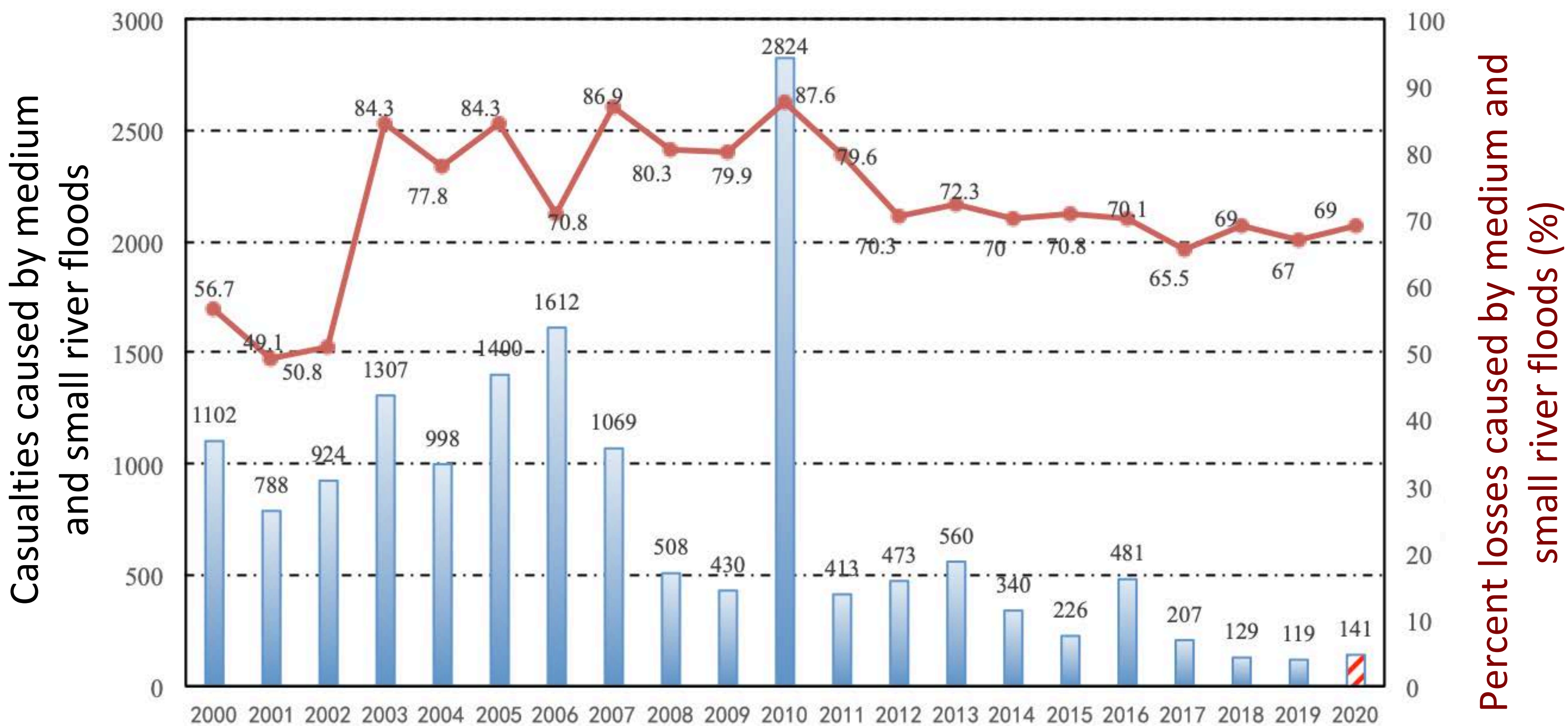

Data from China's Ministry of Water Resources

1. Motivation

Hard for flood forecasting in China’s medium and small river watersheds

- Flood forecasting qualified ratio is relative high in the south, up to 70% or above
- Flood forecasting qualified ratio in the north is only between 40-60%

中华人民共和国水利部
Ministry of Water Resources of the People's Republic of China

China’s Ministry of Water Resources Emphasized the Importance of Flood Forecasting in the Northern Region

海河流域河流产流快，洪水预报难度大，前期部分江河已开始产流，后期降雨产汇流速度会加快。要盯住降雨过程，加强会商分析和监测预警，对永定河、潮白河、滦河、大清河等河流可能出现的涨水过程逐一进行分析，要强化对重点地区的抽查督导，落实落细各项防御措施。前期辽宁部分地区出现不同程度旱情，群众盼水心切，要克服麻痹思想，严防旱涝急转。要重点盯住浑河、太子河、第二松花江等河流，落实各项防御措施。

水利部海河水利委员会
HAIHE RIVER WATER CONSERVANCY COMMISSION, MWR

Haihe River Commission Report

海河流域的防洪问题突出表现在老问题尚未完全解决、新问题更加突出。一方面，多年来国家相继对大中型水库和 15 条主要骨干河道以及中小河流等水利薄弱环节进行治理，但任务尚未全面完成，骨干河道现状防洪标准达标率不足 1/2，小型病险水库（闸）除险加固和蓄滞洪区建设进展迟缓，河道淤障拥塞、堤防老化失修、河口无序开发等造成泄洪能力普遍下降，蓄滞洪区内有近 390 万人缺乏安全避险设施。

1. Motivation

Main reasons of low flood forecasting accuracies for medium and small rivers in the northern regions: limited knowledge on the runoff generation and concentration processes in these regions

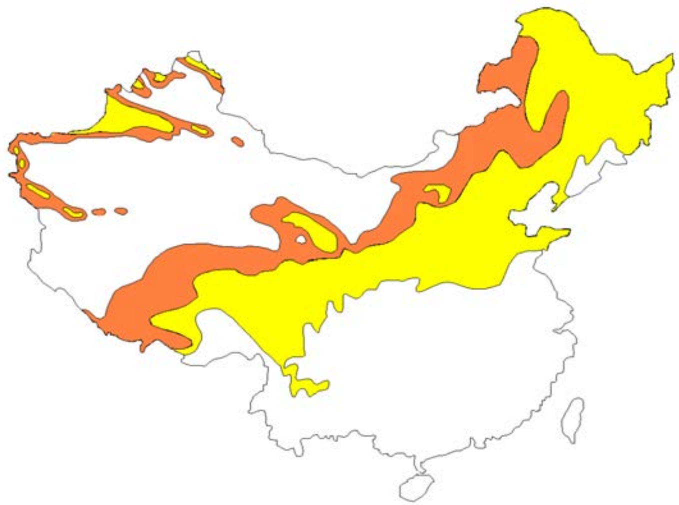

Semi-arid and semi-humid (SASH) regions ≥ 35% of China's territory

- **Humid areas**: Saturation-excess runoff generation is the mode, which has a well established governing equation

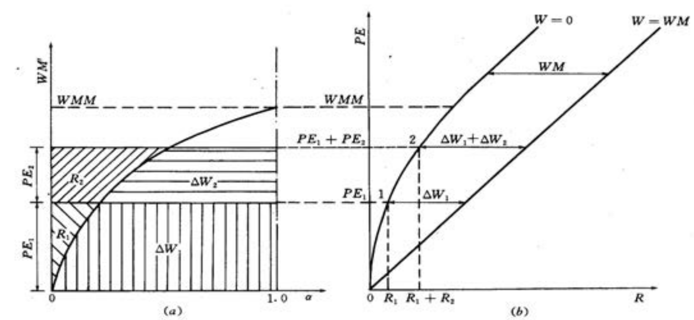

- **Semi-humid and semi arid areas**: Current methods do not work well

Saturation-excess and infiltration-excess may coexist in the SASH areas

1. Motivation

Other important reasons for low flood forecast accuracy in the medium and small rivers:

- ➢ Poor precipitation monitoring & forecasting capabilities
- ➢ Human activities (hydraulic structures construction and groundwater overexploitation) largely altered the land surface conditions

Low precipitation forecasting & monitoring capability

Impacts of hydraulic structures

Groundwater overexploitation

Low station density

Reservoir flood discharge

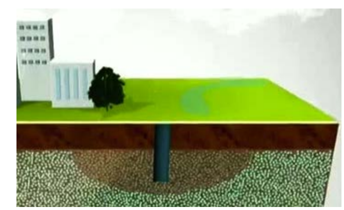

Groundwater depression cone

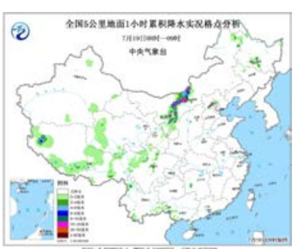

Low forecasting skill

Disturbances on river channel

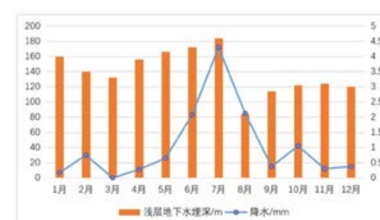

Water level drop

1. Overarching aim and research framework

To enhance flood forecasting capability for medium & small rivers through:

- Combination of fine-scale modelling with multi-source remote sensing
- Accounting for human activities impacts both above and below ground

Improve flood forecasting for medium & small rivers

Forcings	Initial states	Model improvement	
Precipitation multi-source merging and forecasting	Accurate estimation of initial watershed states	Better understanding of runoff yield under different conditions	Better modelling of human disturbances on hydrological processes

2. Multi-source precipitation merging

Sources	Advantages	Disadvantages
Ground Observation	Accurate at site/point level and true ground value	No observations over oceans/remote regions
Satellite QPE	Large (global) coverage, all-weather condition, and good spatial representation	Relative low accuracy (esp. for snowfall) and coarse spatial resolution
Radar QPE	High spatiotemporal resolutions and real-time detection	Limited coverage and impacted by complex terrains
Model QPF	Good spatial coverage and temporally continuous	Relative low quality and poor skill at predicting convective/ fine-scale precipitation

Multi-source precipitation merging has become a popular approach for obtaining high quality precipitation products.

References: Beesley et al., 2009; Hughes, 2006； Adler et al., 2003; Shen et al., 2010

2. Multi-source precipitation merging

A three-step multi-source (satellite/radar/gauge) precipitation merging approach based on mixed geographically weighted regression (MGWR)

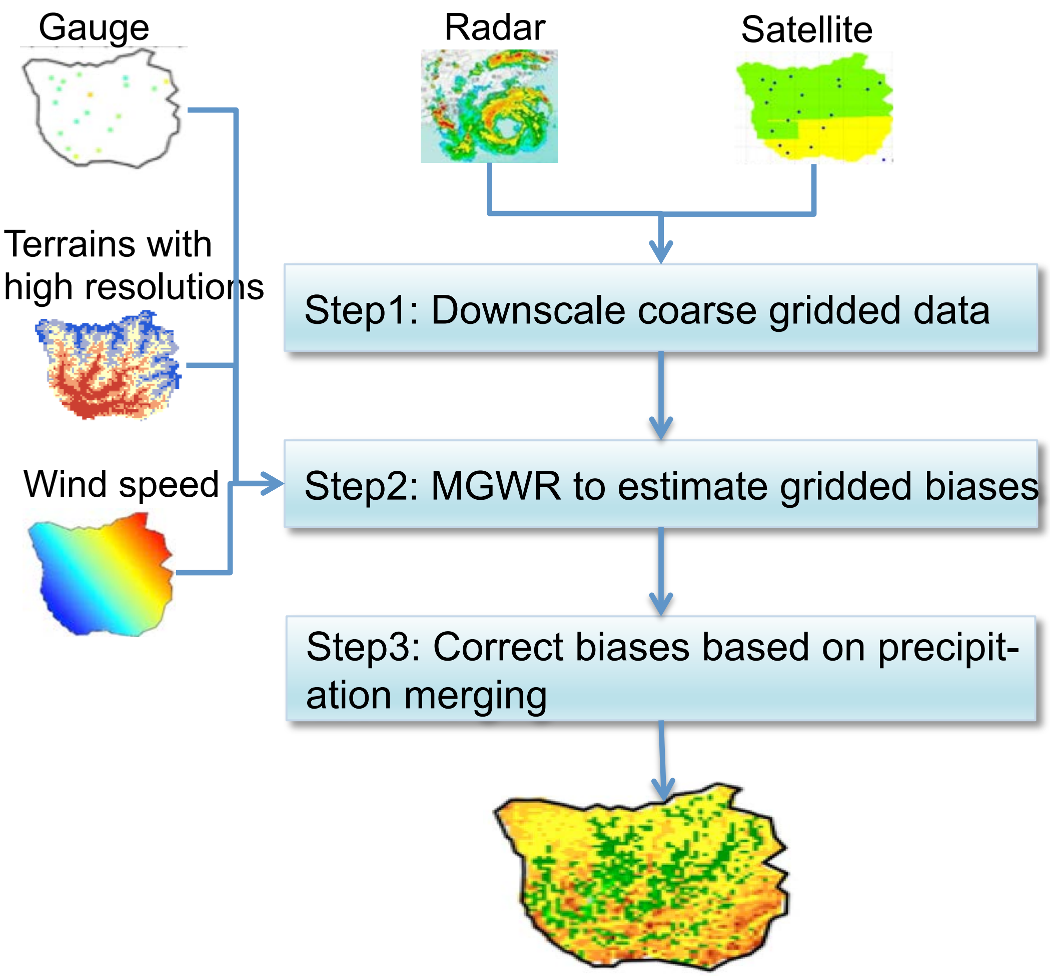

- Mixed geographically weighted regression

$$y_i = \sum_{k=1}^{n_1} a_{ik} x_{ik}(a) + \sum_{l=1}^{n_2} b_l x_{il}(b) + \theta_i$$

- Spatial weighting functions

✓ Threshold $w_{ij} = \begin{cases} 1 & d_{ij} \leq D \\ 0 & d_{ij} > D \end{cases}$

✓ Inverse distance $w_{ij} = 1/d_{ij}^{\alpha}$

✓ Gauss $w_{ij} = \exp(-(d_{ij}/b))^2$

✓ Bi-square $w_{ij} = \begin{cases} [1-(d_{ij}/b)^2]^2 & d_{ij} \leq b \\ 0 & d_{ij} > b \end{cases}$

References: Chao, †Zhang, et al. (2018), Geographically Weighted Regression Based Methods For Merging Satellite and Gauge Precipitation *Journal of Hydrology*, 558, 275-289.

2. Multi-source precipitation merging

Hanjiang’s Tributary

-- Ziwuhe Watershed

Original CMORPH satellite QPE
(20130523 event）

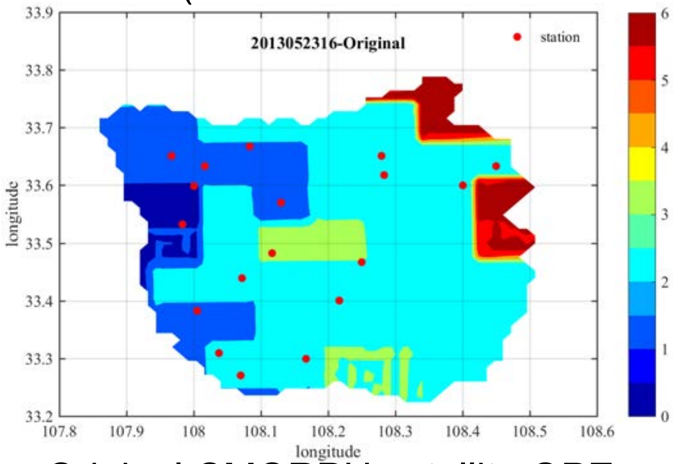

Merged precipitation
（20130523 event）

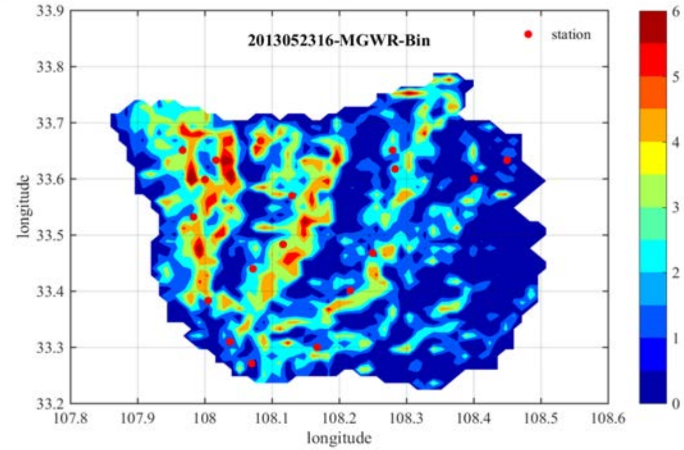

Original CMORPH satellite QPE
(Hourly precipitation of 2013)

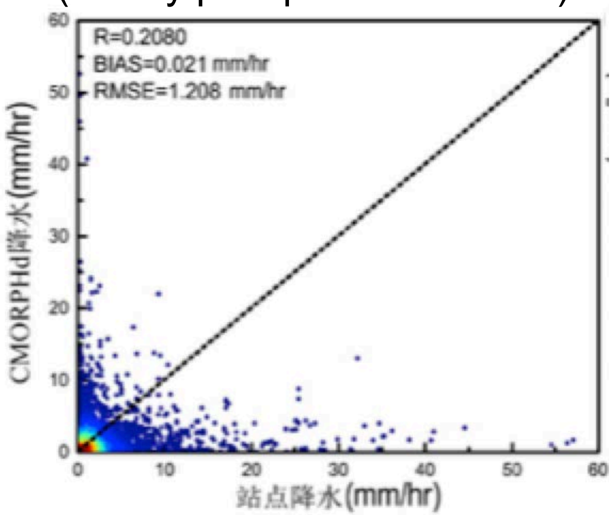

Merged precipitation
（Hourly precipitation of 2013 ）

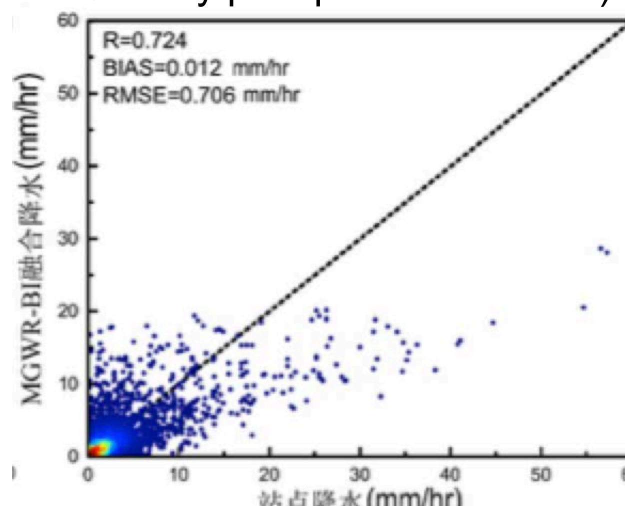

References: Chao, †Zhang, et al. (2018), Geographically Weighted Regression Based Methods For Merging Satellite and Gauge Precipitation *Journal of Hydrology*, 558, 275-289.

2. Multi-source precipitation merging

Application of multi-source precipitation merging in the flood forecasting by the WRF-Hydro model based on land-atmosphere coupling

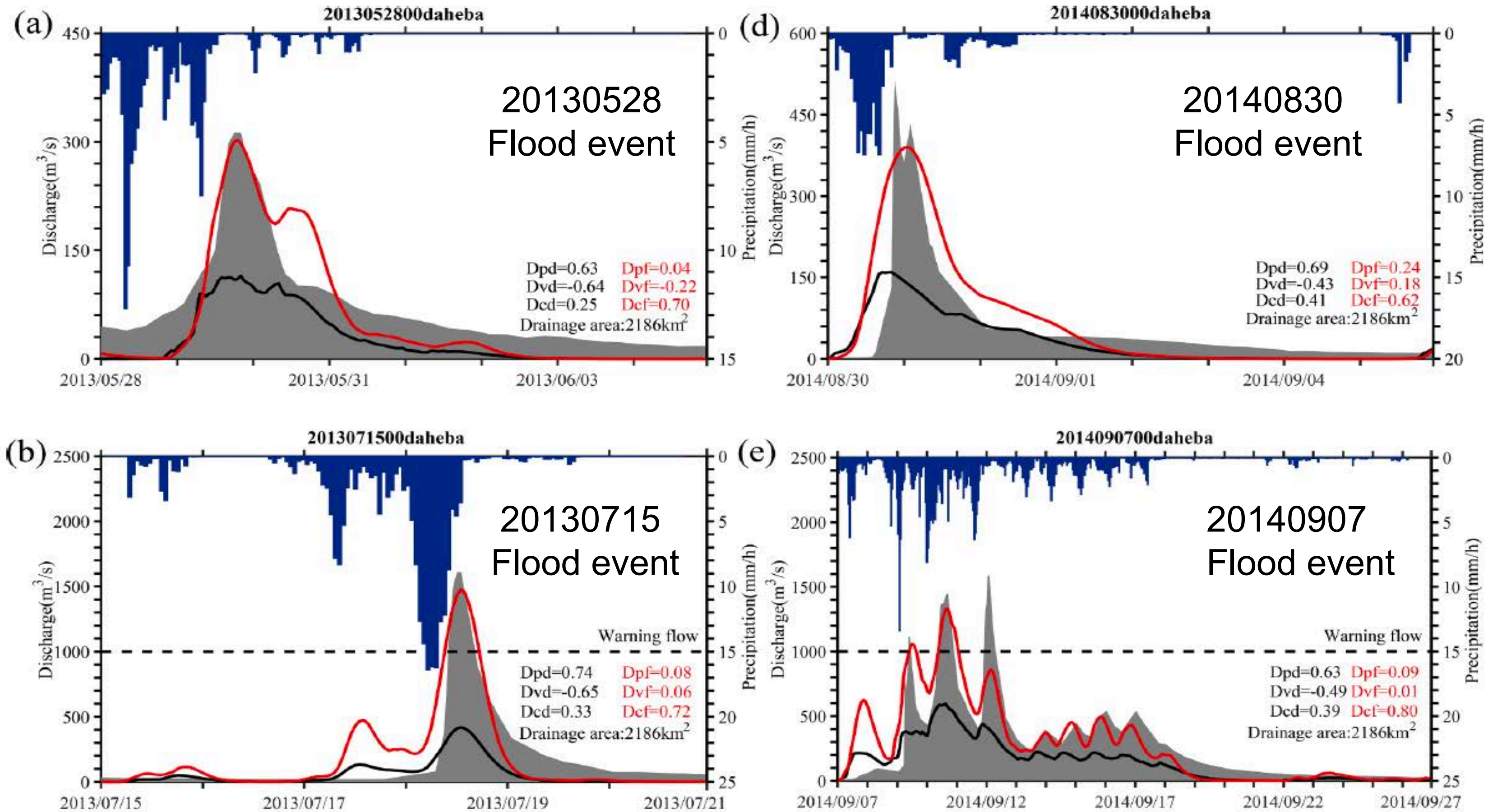

Black line: simulated hydrograph driven by WRF precipitation forecasting

Red line: simulated hydrograph driven by ground-model merged precipitation

References: Chao, †Zhang, et al. (2020). Improving flood simulation capability of the WRF-Hydro-RAPID model using a multi-source precipitation merging method, *Journal of Hydrology*, 592, 125814.

3. Remote sensing of watershed states

Soil moisture remote sensing

Satellites	Bands	Operating Period	Resolutions
SMAP	1.41 GHz	2015.03-present	36 km
SMOS	1.413 GHz	2010.06-present	25 km
Fengyun (FY)	10-36 GHz	2011.07-present	25 km
AMSR2	10-89 GHz	2012.07-present	10 & 25 km

SMAP

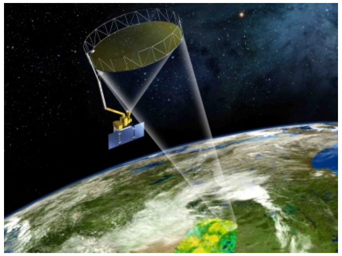

SMOS

FY3B

AMSR2

3. Remote sensing of watershed states

Soil moisture remote sensing

SMAP
(2015-06-01)

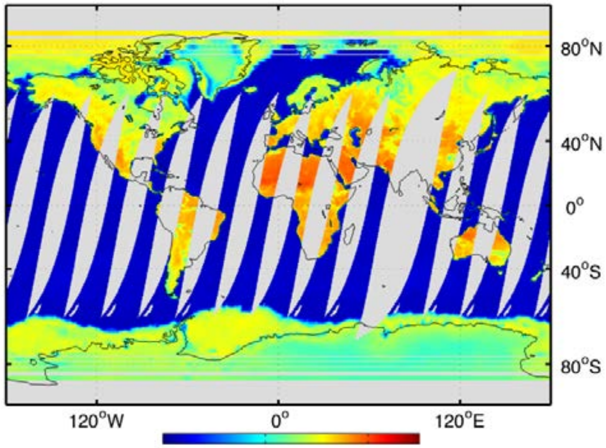

SMOS
(2015-06-01)

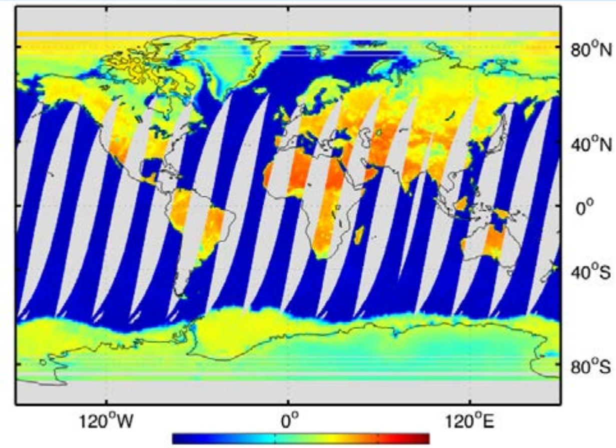

FY3B
(2015-06-01)

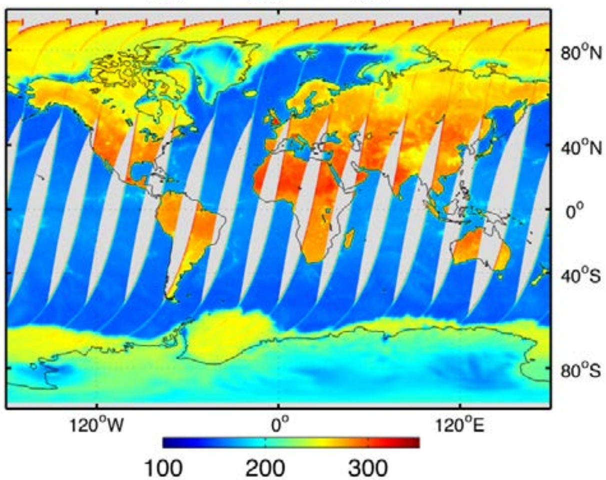

AMSR2
(2015-06-01)

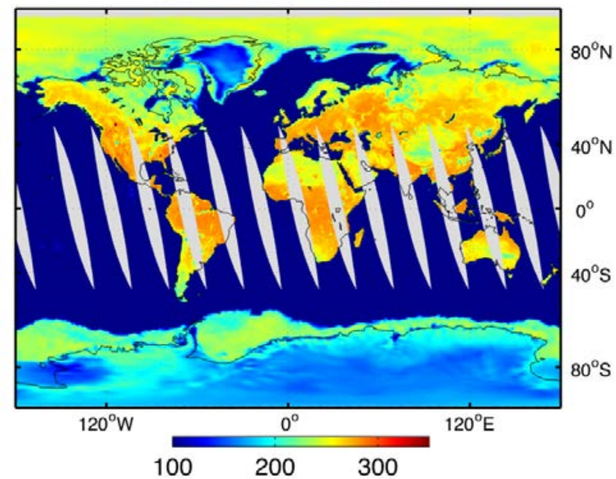

- None of these satellites can provide seamless observations of T_b globally and across China;
- Retrieval algorithms of these satellite SWC products differ among each other.

References: Zhang, et al. (2019). Using multi-satellite microwave remote sensing observations for retrieval of daily surface soil moisture across China, *Water Science and Engineering*, 12(2): 85-97.

3. Remote sensing of watershed states

Soil moisture remote sensing

Step 1: Retrieval

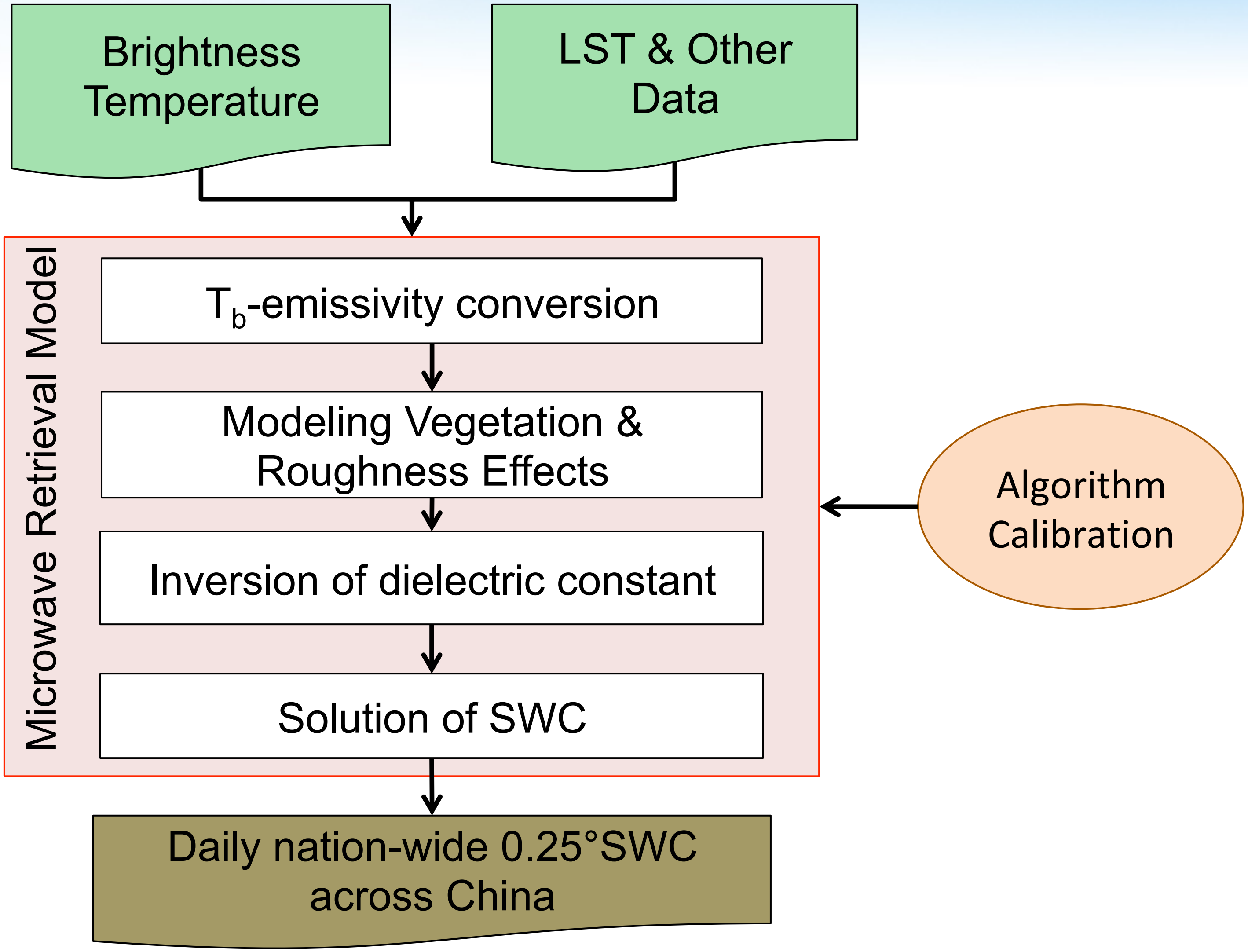

References: (1) Zhang, et al. (2019). Using multi-satellite microwave remote sensing observations for retrieval of daily surface soil moisture across China, *Water Science and Engineering*, 12(2): 85-97.
(2) China Inventions Patent：A multi-source satellite soil moisture retrieval method，No. ZL201810473645.5

3. Remote sensing of watershed states

Soil moisture remote sensing

Step 2: Downscaling

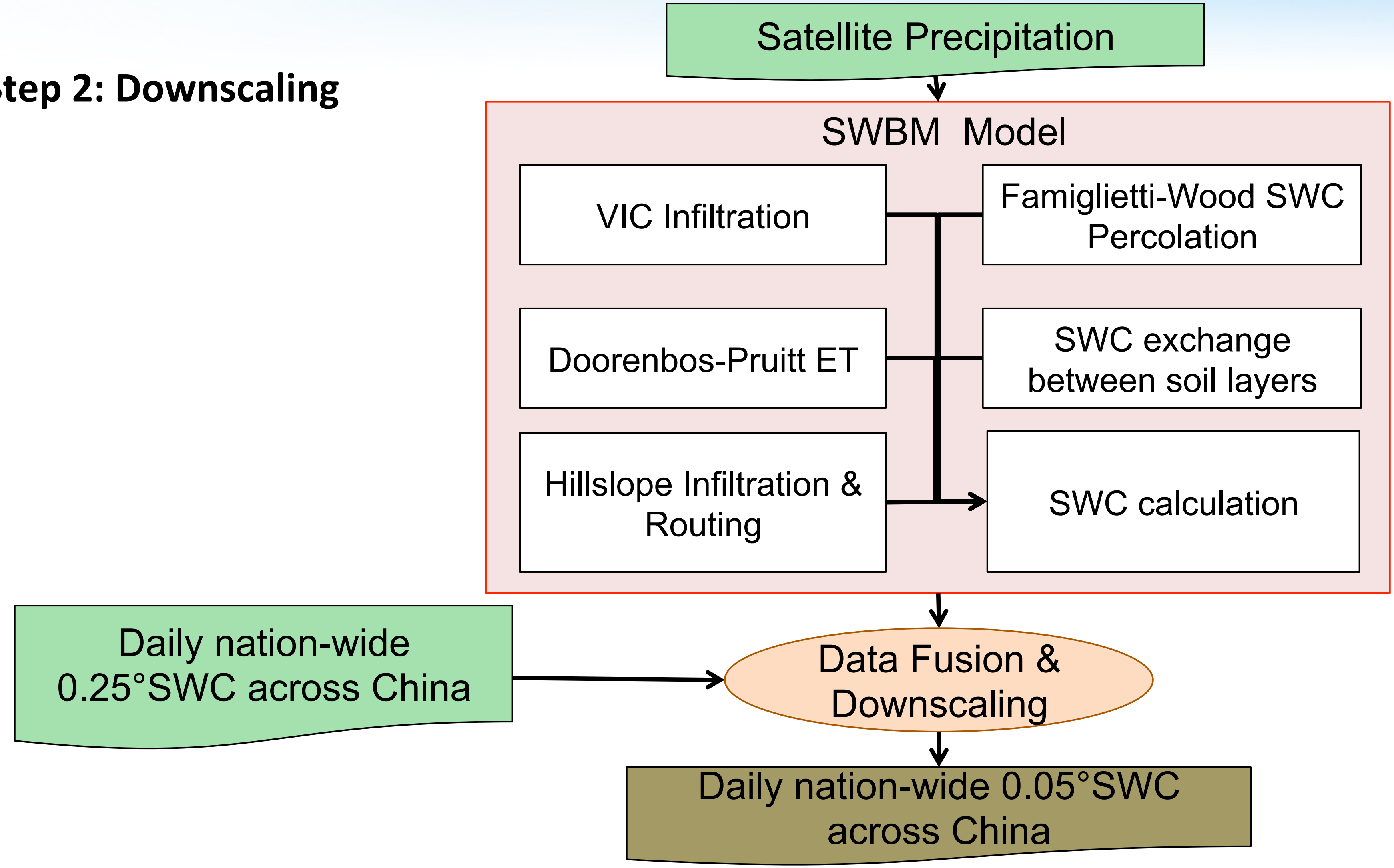

References: (1) Zhang, et al. (2019). Using multi-satellite microwave remote sensing observations for retrieval of daily surface soil moisture across China, *Water Science and Engineering*, 12(2): 85-97.

(2) China Inventions Patent：A multi-source satellite soil moisture retrieval method，No. ZL201810473645.5

3. Remote sensing of watershed states

Soil moisture remote sensing

Site-level validation

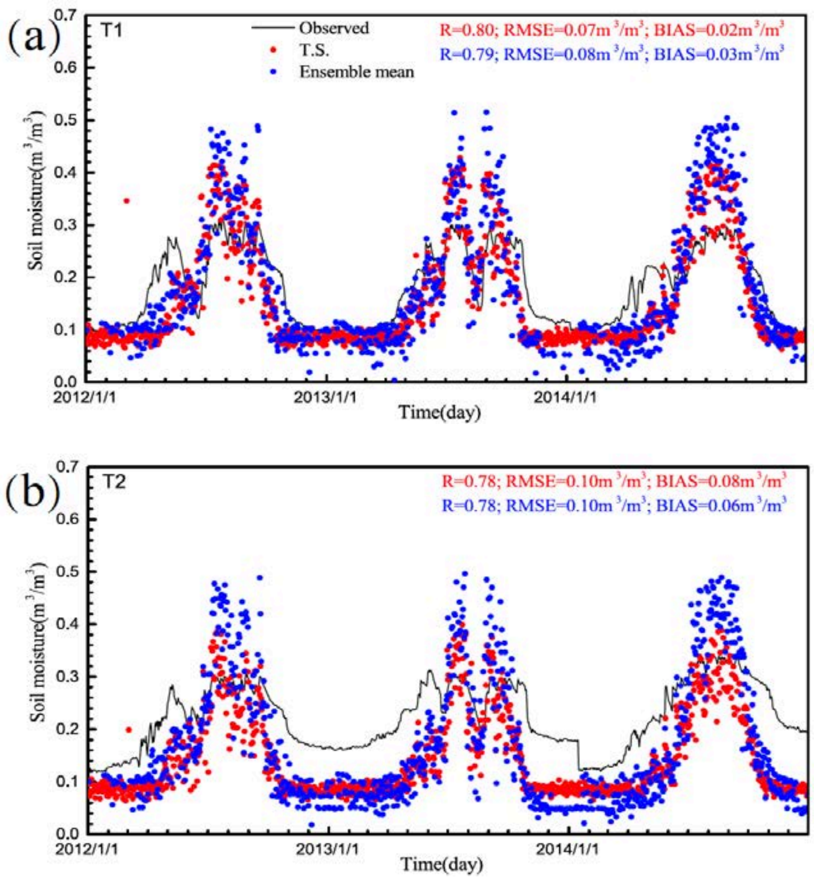

Seasonality of retrieved SM from 2000-2020

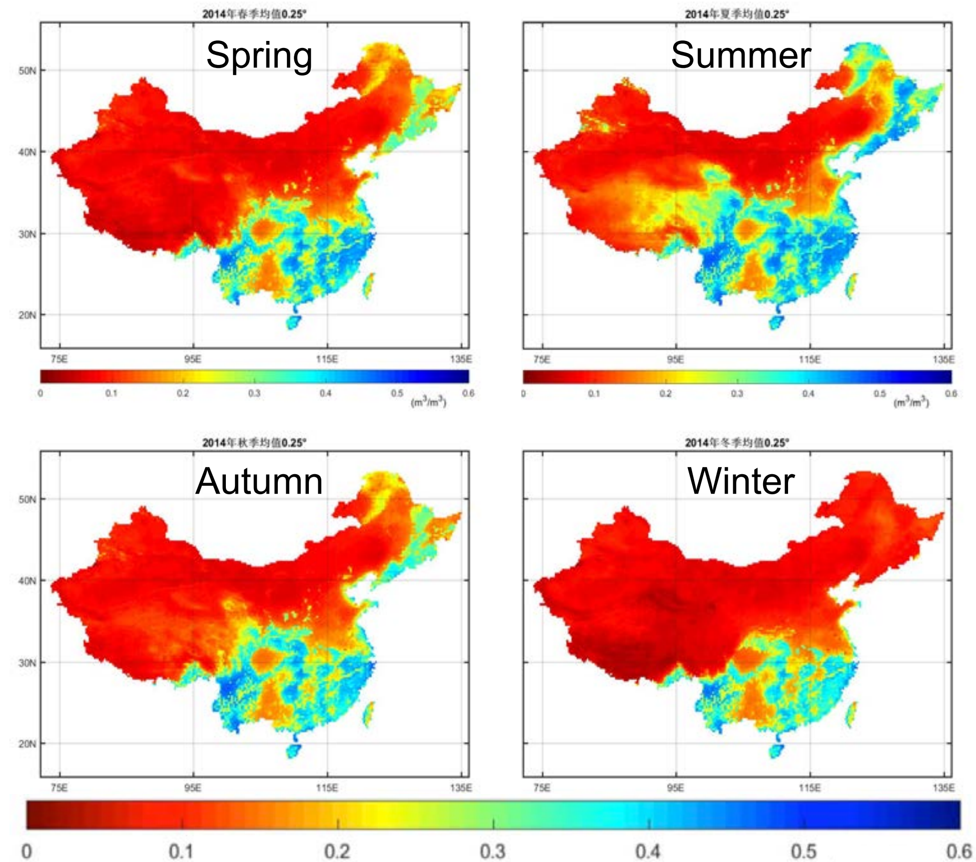

Land surface soil moisture (m³/m³)

†Zhang, Chao, Wang, et al. (2019). Using multi-satellite microwave remote sensing observations for retrieval of daily surface soil moisture across China, *Water Science and Engineering*, 12(2): 85-97.

Liu, R., †**K. Zhang**, et al. (2017). Analysis of spatiotemporal characteristics of surface soil moisture across China based on multi-satellite observations, *Advances in Water Science*, 28(4), 479-487.

3. Remote sensing of watershed states

Remote sensing of hydraulic structure water storage

Extraction of reservoir water body

Removal of hill/mountain shadows

- Size and location of shadow depend on the zenith angle, latitude, longitude, and hill slope

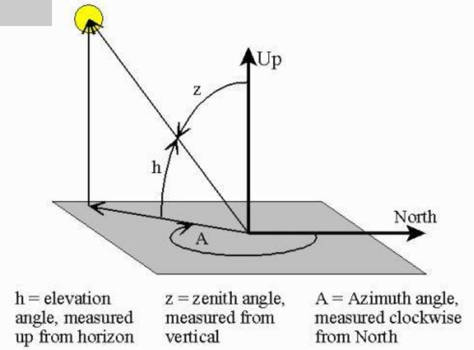

$$Hiishade = \left(cos(Zenith\_rad) * cos(Slope\_rad)\right) + \left(sin(Zenith\_rad) * sin(Slope\_rad) * cos(Azimuth\_rad - Aspect\_rad)\right)$$

Delineation of boundary buffer zone

- Structure A is dilated by structure B

$$A \oplus B = \{z \mid (B\hat{})z \cap A \neq \emptyset\}$$

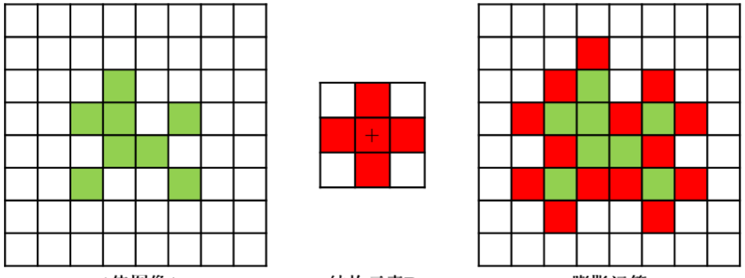

- Structure A is eroded by structure B

$$A \odot B = \{z \mid (B)z \subseteq A\}$$

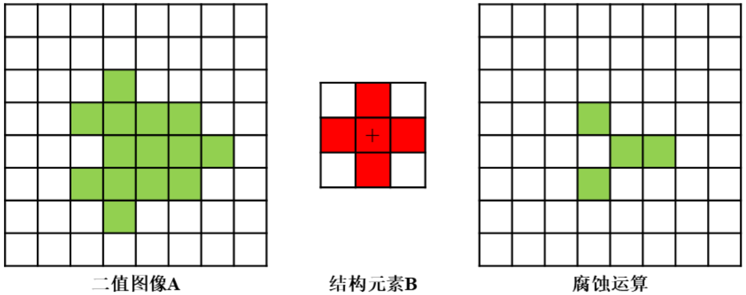

Fan et al. (2021). Optimal extraction of reservoir water body from remote sensing images based on iterative inter-class variance maximization method, *Water Resources Protection*, 37(3), 50-55+60.

3. Remote sensing of watershed states

Soil moisture remote sensing

Delineation of water body boundary: we developed an iterative inter-class variance maximization method based on Otsu's inter-class variance maximization method

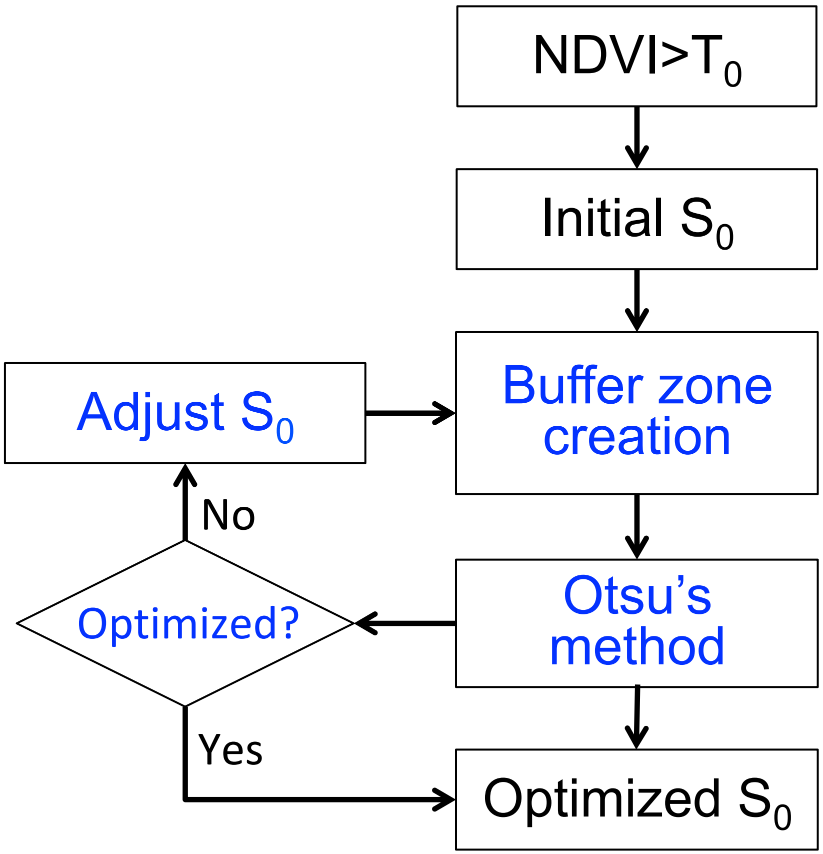

$$p_i = \frac{K_i}{M \times N}, \quad i = 0,1,2,\cdots,255$$

$$\omega_0 = \frac{N_0}{M \times N}$$

$$\omega_1 = \frac{N_1}{M \times N}$$

$$\omega 0 + \omega 1 = 1$$

$$\mu_0 = \sum_{i=0}^{T} \frac{i \times p_i}{\omega_0}$$

$$\mu_1 = \sum_{i=T+1}^{255} \frac{i \times p_i}{\omega_1}$$

$$\mu = \omega_0 \mu_0 + \omega_1 \mu_1$$

$$G = \omega_0 (\mu_0 - \mu)^2 + \omega_1 (\mu_1 - \mu)^2$$

Fan et al. (2021). Optimal extraction of reservoir water body from remote sensing images based on iterative inter-class variance maximization method, *Water Resources Protection*, 37(3), 50-55+60.

Improvement on infiltration-excess model

Green-Ampt model

The Green-Ampt rainfall-runoff model is an infiltration-excess rainfall-runoff model based on the Green-Ampt infiltration equation.

The Green-Ampt infiltration equation is written as:

$$f(t) = K\left[1 + \frac{\psi \Delta\theta}{F(t)}\right]$$

$f(t)$ — infiltration capacity;

K — the saturated hydraulic conductivity;

ψ — the wetting front capillary pressure head;

$\Delta\theta$ — the change of soil water content across the wetting front;

$F(t)$ — the cumulative infiltration。

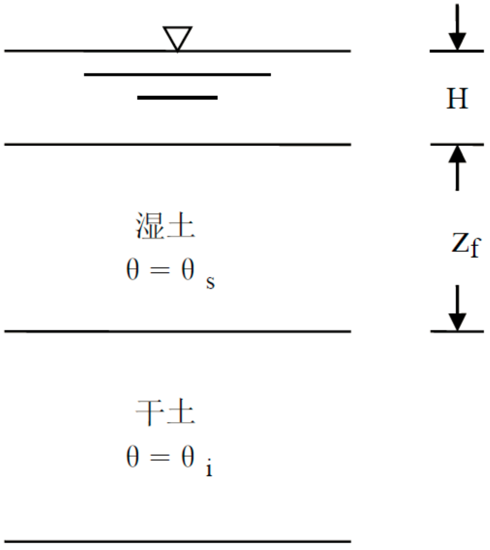

Green-Ampt model

Improvement on infiltration-excess model

Empirical (conceptualized) infiltration capacity distribution curve

$$\frac{a}{A} = 1 - \left(1 - \frac{f'_m}{f_{mm}}\right)^B$$

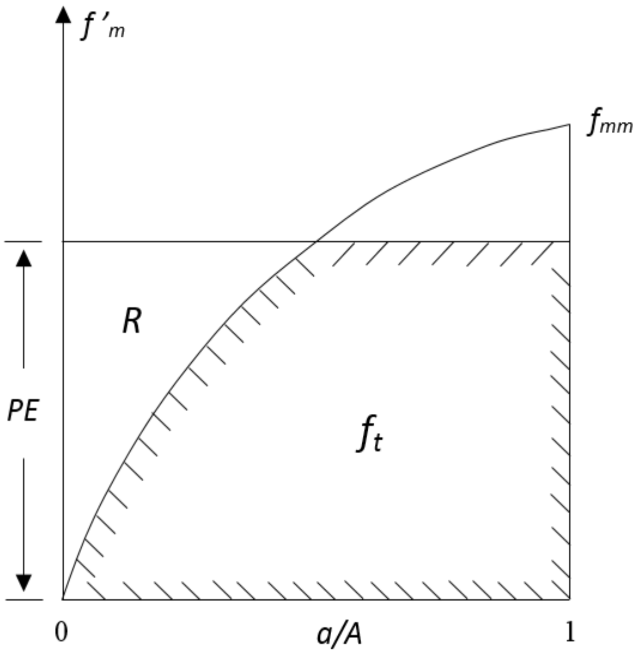

The distribution curve of infiltration capacity for the Green-Ampt rainfall-runoff model.

PURPOSES :

Consider the spatial heterogeneity of infiltration capacity

ISSUE :

1. Is the real infiltration curve a parabola?
2. Is the shape of the curve fixed?

Improvement on infiltration-excess model

"Close to reality" infiltration capacity distribution curve

The values of the parameters for the Green-Ampt model relate to the soil type, including total porosity, effective porosity, wetting front capillary pressure head, and saturated hydraulic conductivity.

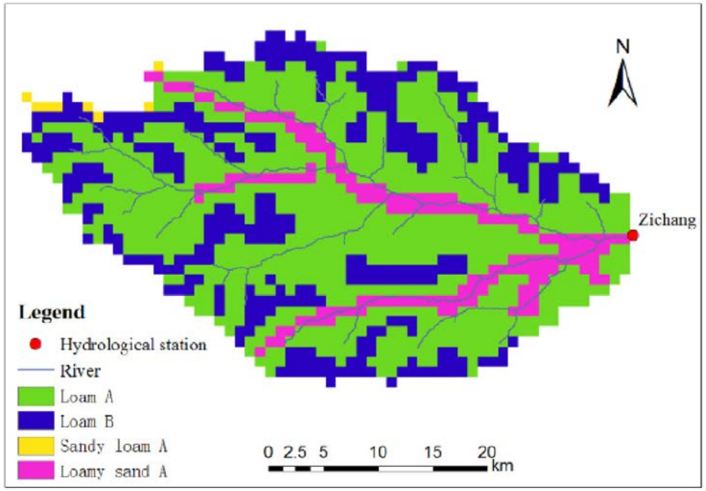

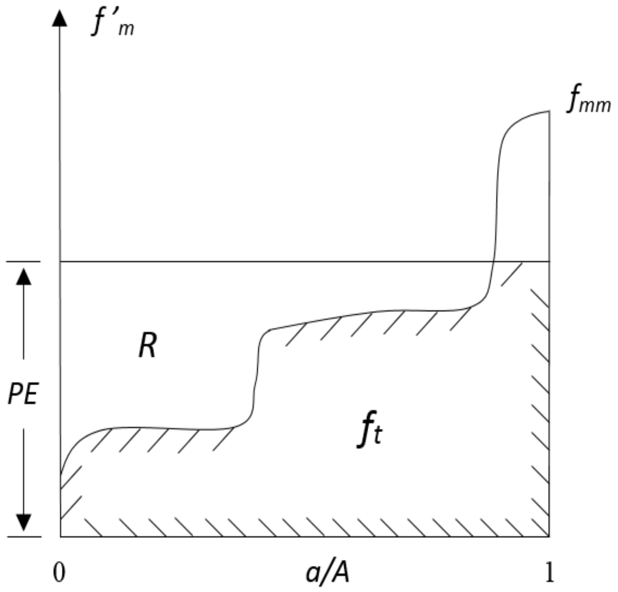

The physically based infiltration distribution curve

Huo, †Li, †Zhang, et al.(2020). GA-PIC: an improved Green-Ampt rainfall-runoff model with a physically based infiltration distribution curve for semi-arid basins, *Journal of Hydrology*, 586, 124900.

4. Modelling of runoff yield and concentration

Improvement on infiltration-excess model

- **Comparison of two Infiltration curves in the Caoping Watershed**

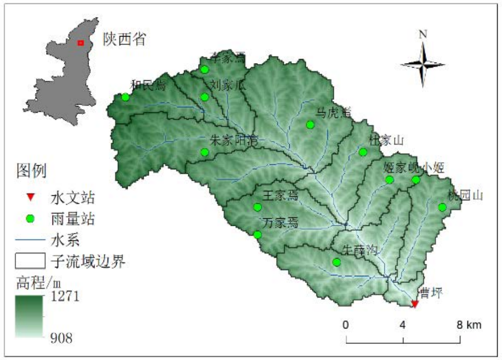

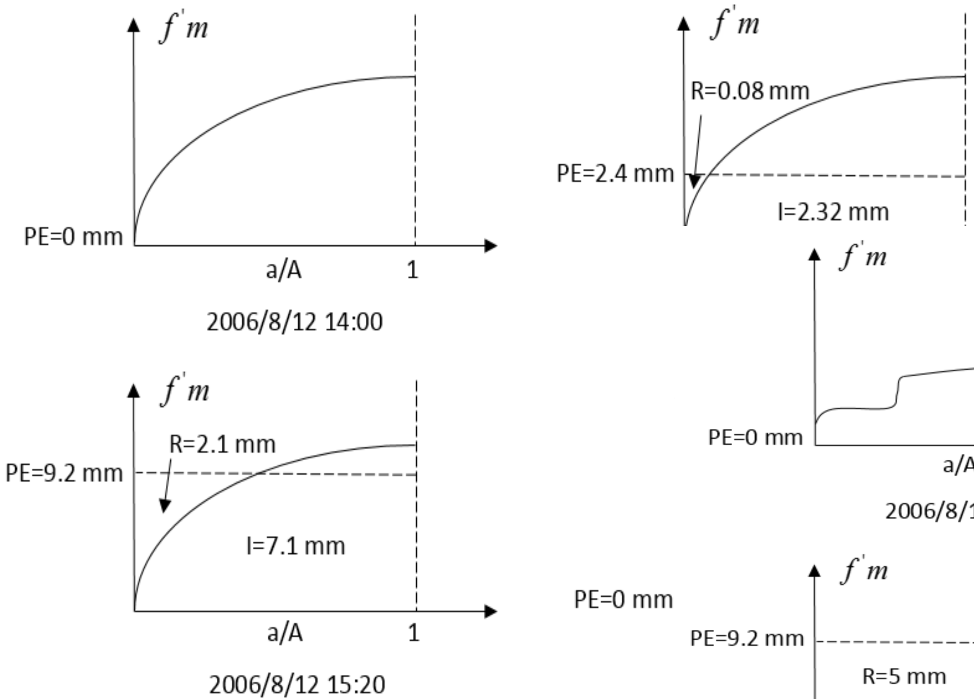

The empirical infiltration capacity curve in GA model

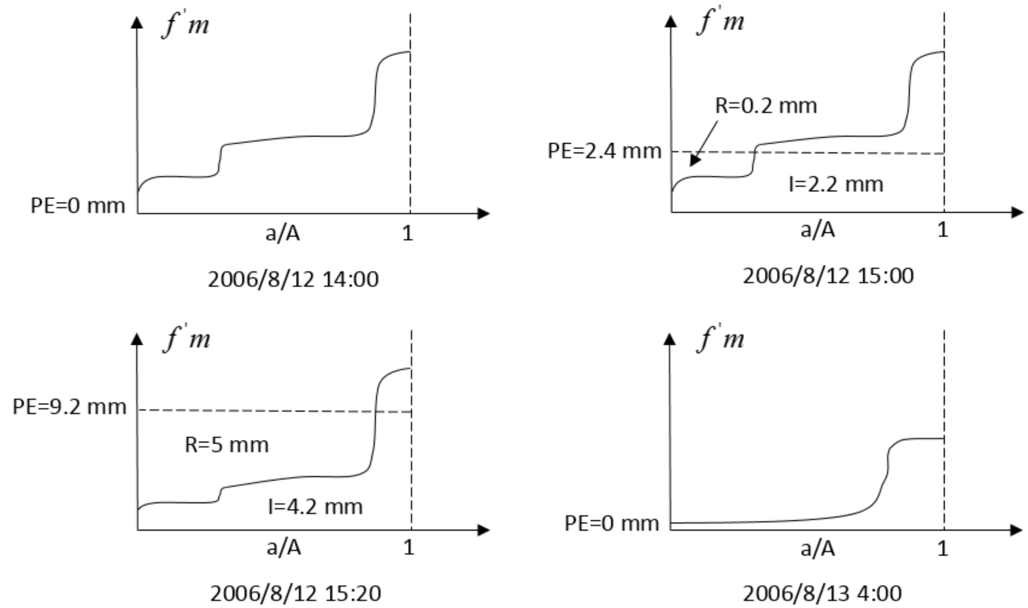

The physically based infiltration distribution curve in GA-PIC model

Huo, †Li, †Zhang, et al.(2020). GA-PIC: an improved Green-Ampt rainfall-runoff model with a physically based infiltration distribution curve for semi-arid basins, *Journal of Hydrology*, 586, 124900.

4. Modelling of runoff yield and concentration

Runoff yield modes

Spatial combination computing models

A watershed is divided into SED and IED sub-watersheds using the CN-TI method.

- **Curve number (CN)** is the only parameter of the SCS-CN model that characterizes the tendency of infiltration-excess runoff generation. Larger CN value means high likeliness of infiltration-excess
- **Topographic Index (TI)** acts as a quantitative measure of topography impact on saturation-excess runoff generation. Larger TI value indicates higher probability of saturation-excess

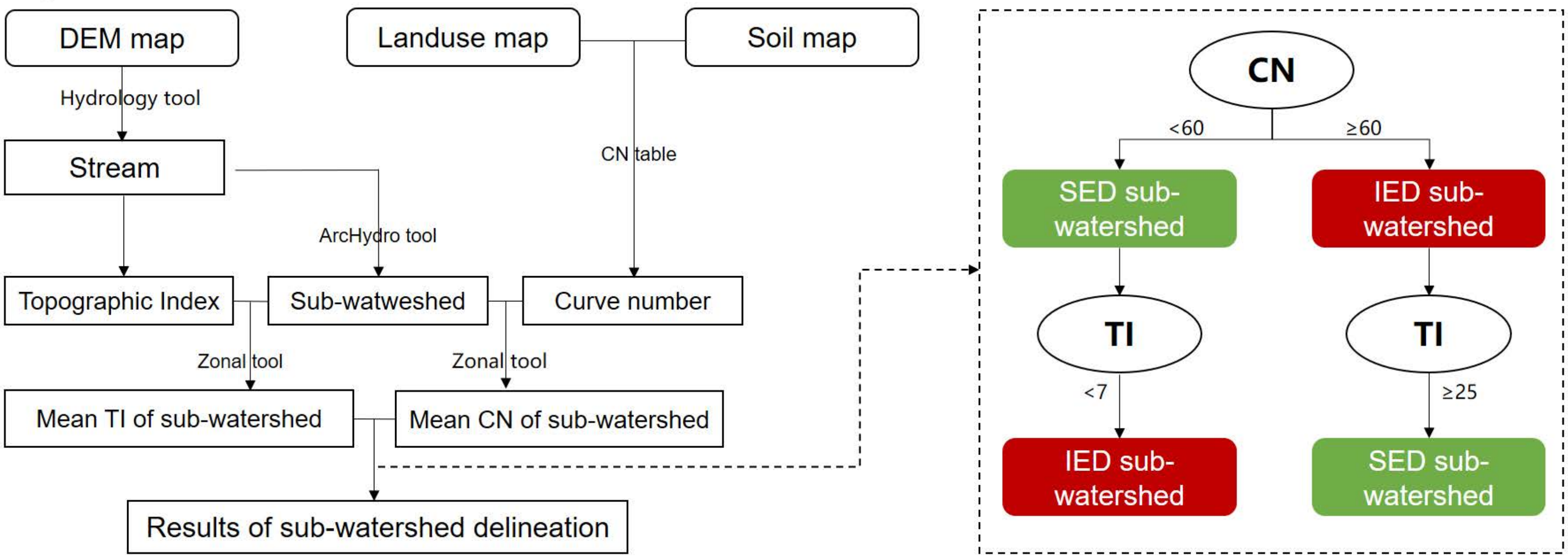

Liu, †Zhang, †Li, et al.(2020). A hybrid runoff generation modelling framework based on spatial combination of three runoff generation schemes for semi-humid and semi-arid watersheds, *Journal of Hydrology*, 290, 125440.

4. Modelling of runoff yield and concentration

Runoff yield modes

Spatial combination computing models (SCCMs)

Three classical runoff generation schemes were selected, including the Xinanjiang saturation-excess scheme, Green-Ampt, and Xinanjiang-Green Ampt scheme. Based on the given types of sub-watersheds, the combination of the three schemes can lead to six valid combinations that are referred to as the SCCMs.

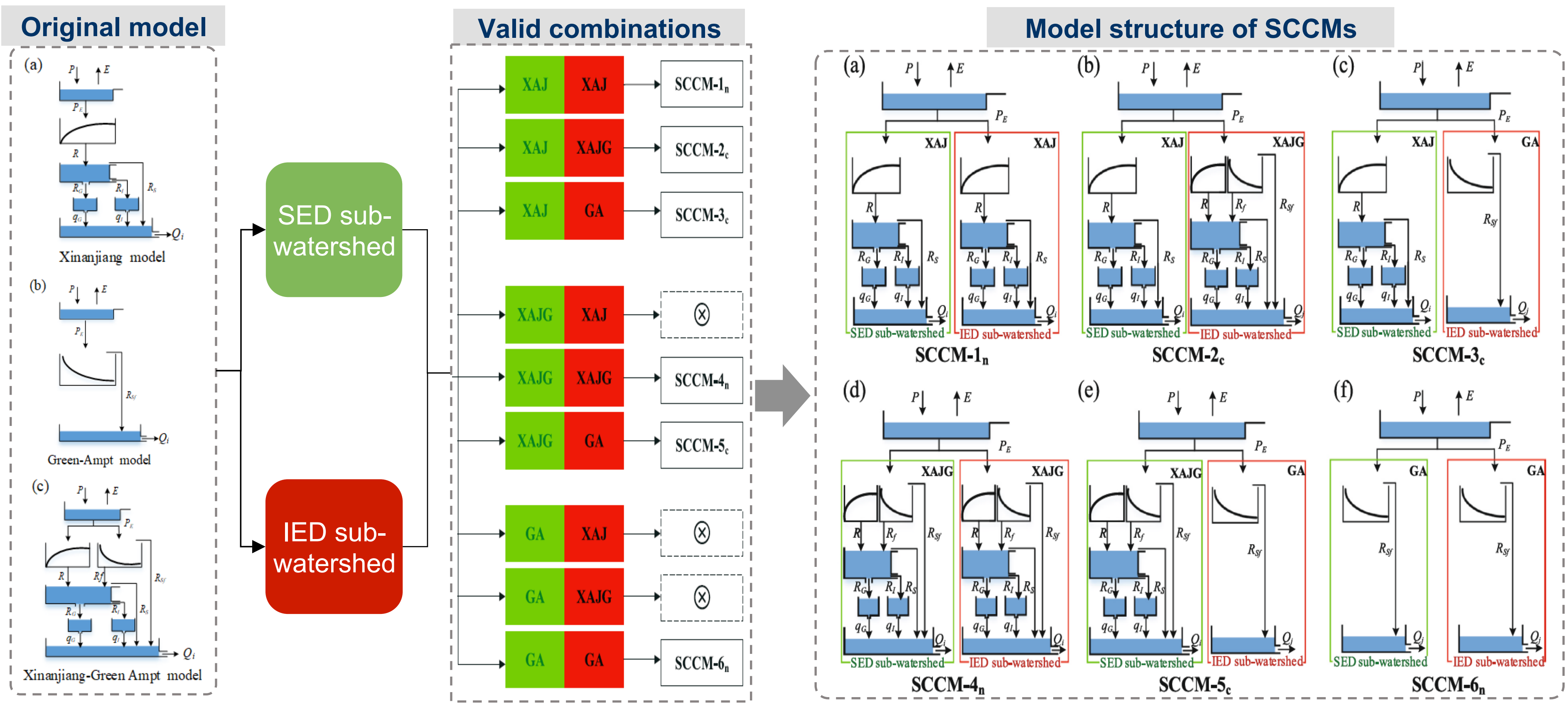

Liu, †Zhang, †Li, et al.(2020). A hybrid runoff generation modelling framework based on spatial combination of three runoff generation schemes for semi-humid and semi-arid watersheds, *Journal of Hydrology*, 290, 125440.

4. Modelling of runoff yield and concentration

Model Integration

Dual anthropogenic aboveground and underground regulation

- Account for the spatial impacts of human activities based on water conservancy project and groundwater depth distribution
- Quantify the reduction effects of water conservancy projects and groundwater overexploitation on runoff by introducing spatial and temporal storage reservoirs

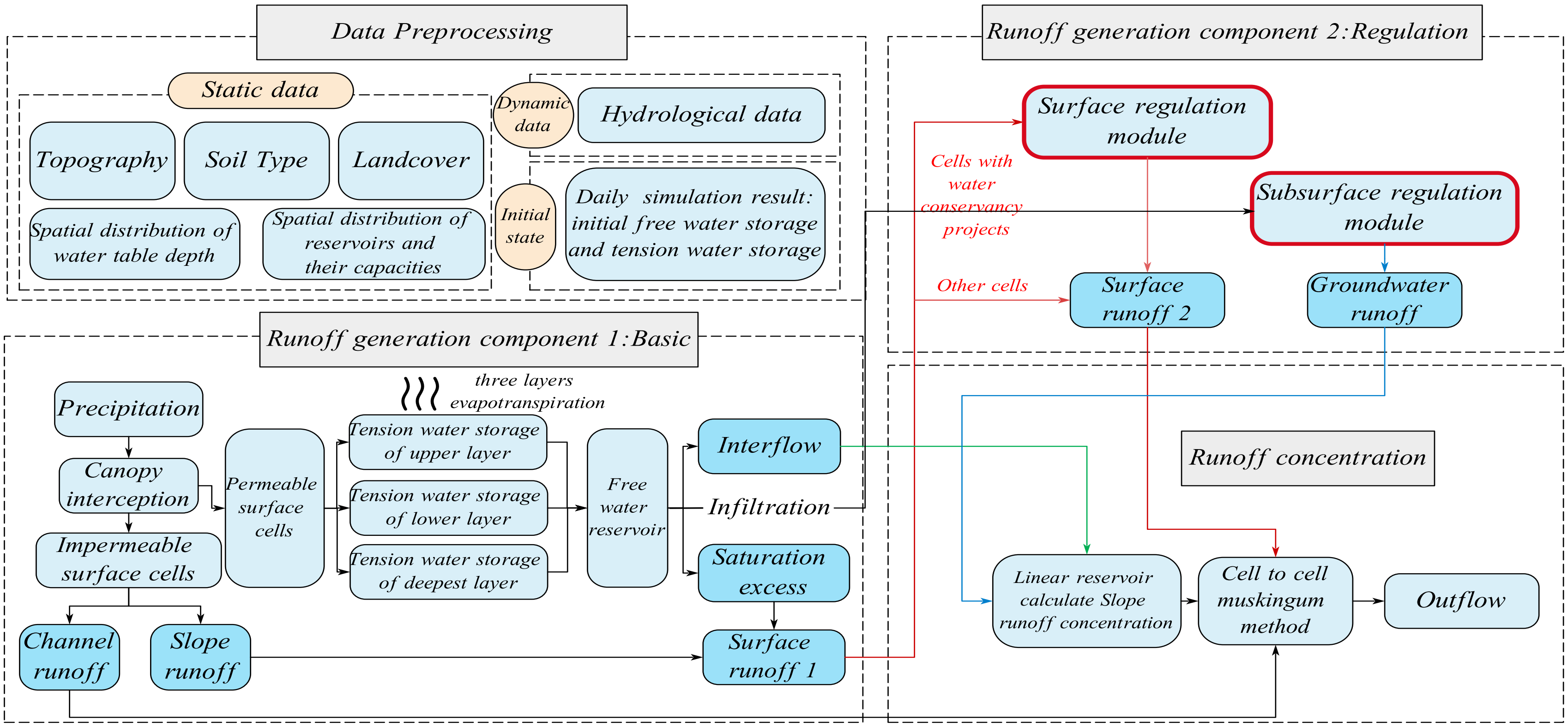

Zhang et al. (2021). Gridded Xin'anjiang-dual anthropogenic aboveground and underground regulation distributed hydrological model, *Water Resources Protection*, 37(5), 94-101

Dual anthropogenic aboveground and underground regulation —underground regulation

Underground anthropogenic regulation

S is the "threshold" that affects the underground runoff in the water source division. Only when the free water depth in the soil is greater than S_0, groundwater runoff occurs.

- This structure is equivalent to the increase of free water storage reservoir capacity ($S_m + S_0$), which reduces the surface runoff

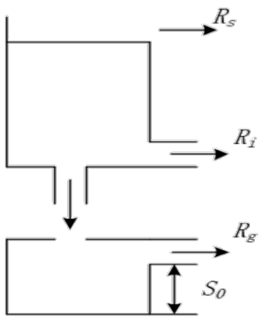

$Z_{river} > Z_{impervious\ layer} > Z_{groundwater}$

$S_0 = (Z_{river} - Z_{impervious\ layer}) \times n$

$Z_{river} > Z_{groundwater} > Z_{impervious\ layer}$

$S_0 = (Z_{river} - Z_{groundwater}) \times n$

$Z_{groundwater} > Z_{river}$

$S_0 = 0$

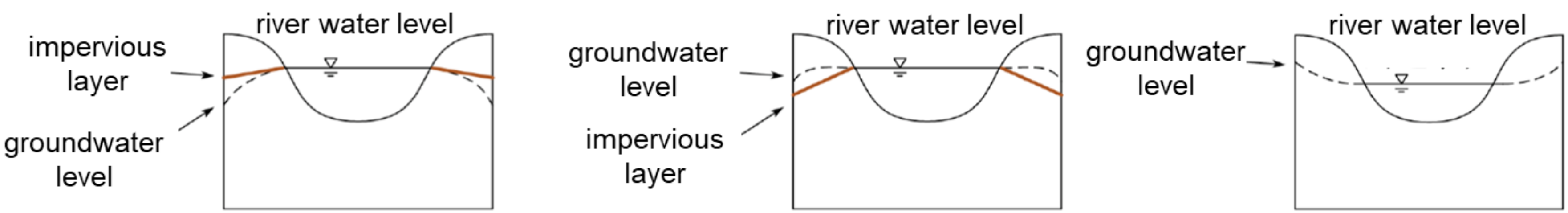

Huang et al., JMS, 2017; Zhang et al, Water Resources Protection, 2021

4. Modelling of runoff yield and concentration

Case study

Overview of the Qingshui River Watershed

- Watershed area: 1650km^2
- Multi-year average annual precipitation: 457.1mm
- Multi-year average annual runoff: 29 million m^3 (176 mm/yr) (1971-2010)

Location and station distribution of the Qingshui River Watershed

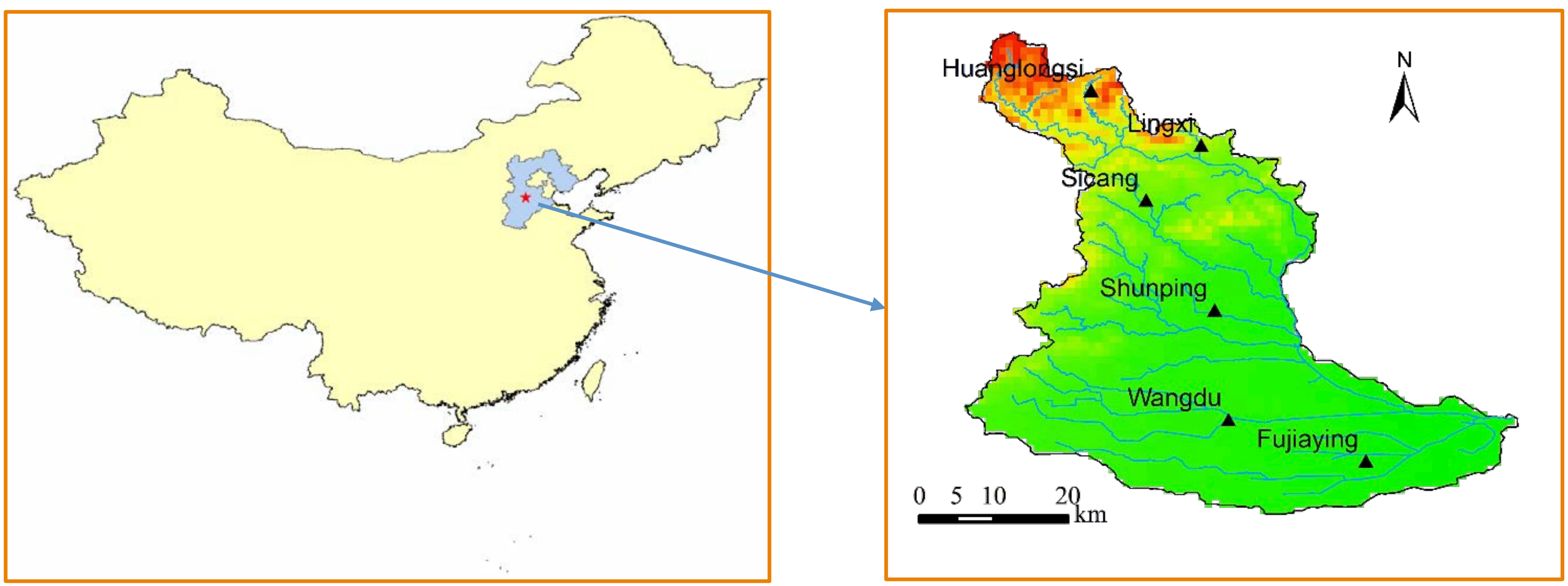

4. Modelling of runoff yield and concentration

Case study

Underlying surface conditions

- DEM、landcover、soil (0-30cm、30-100cm) 、topographic index、cumulative catchment area

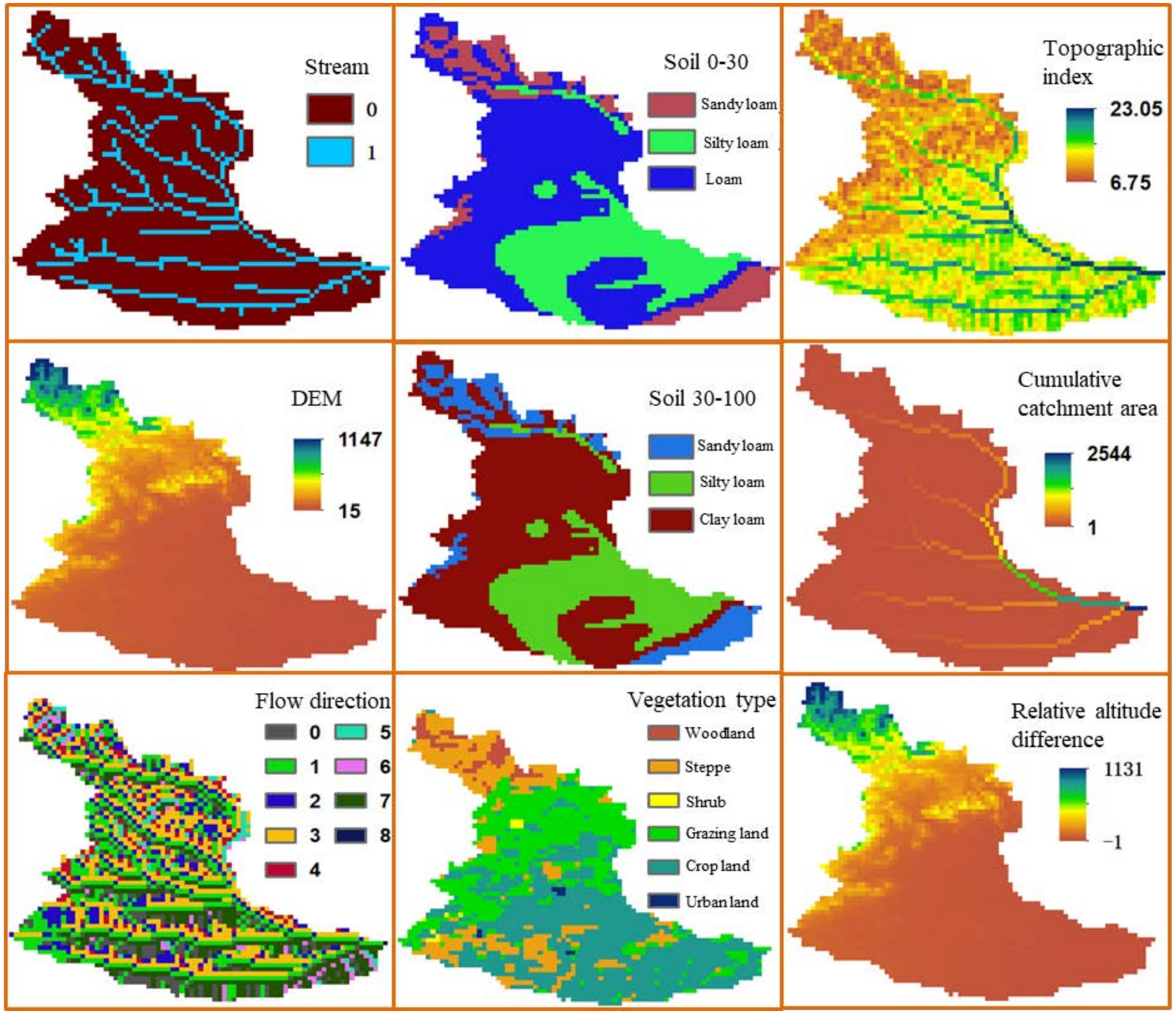

4. Modelling of runoff yield and concentration

Case study

Hydrological data

Hydrological element	Time period	Number of the station	Temporal resolustion
Precipitation	1966-2018	7	daily, hourly
Evaporation	1966-2018	1	daily
Discharge	1966-2018	1	daily, hourly
Soil moisture	2010-2019	5	every 10 days
Groundwater level	2010-2018	13	daily
River water level	2010-2018	1	daily
Water temperature	2010-2018	1	daily
Vapor pressure	2010-2018	1	daily
Wind speed	2010-2018	1	daily
……	……	……	

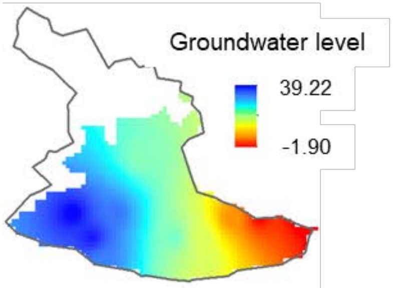

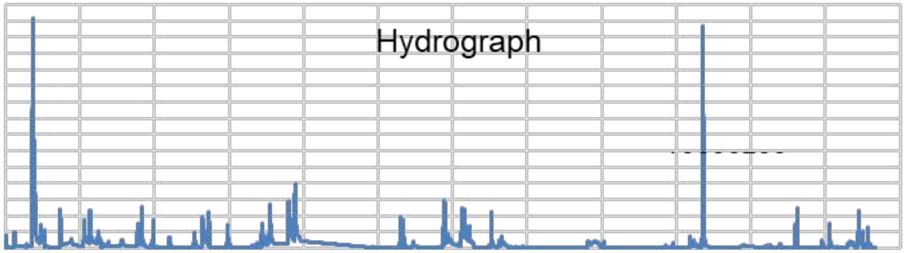

4. Modelling of runoff yield and concentration

Case study

Overview of water conservancy projects

- One Medium-sized reservoir: Longtan Reservoir in the upper reaches of Qingshui River
- Seven small reservoirs: Xixiankou Reservoir, Beigucheng Reservoir, Nangucheng Reservoir, etc, in Tang County
- One pond：Shuitou Reservoir

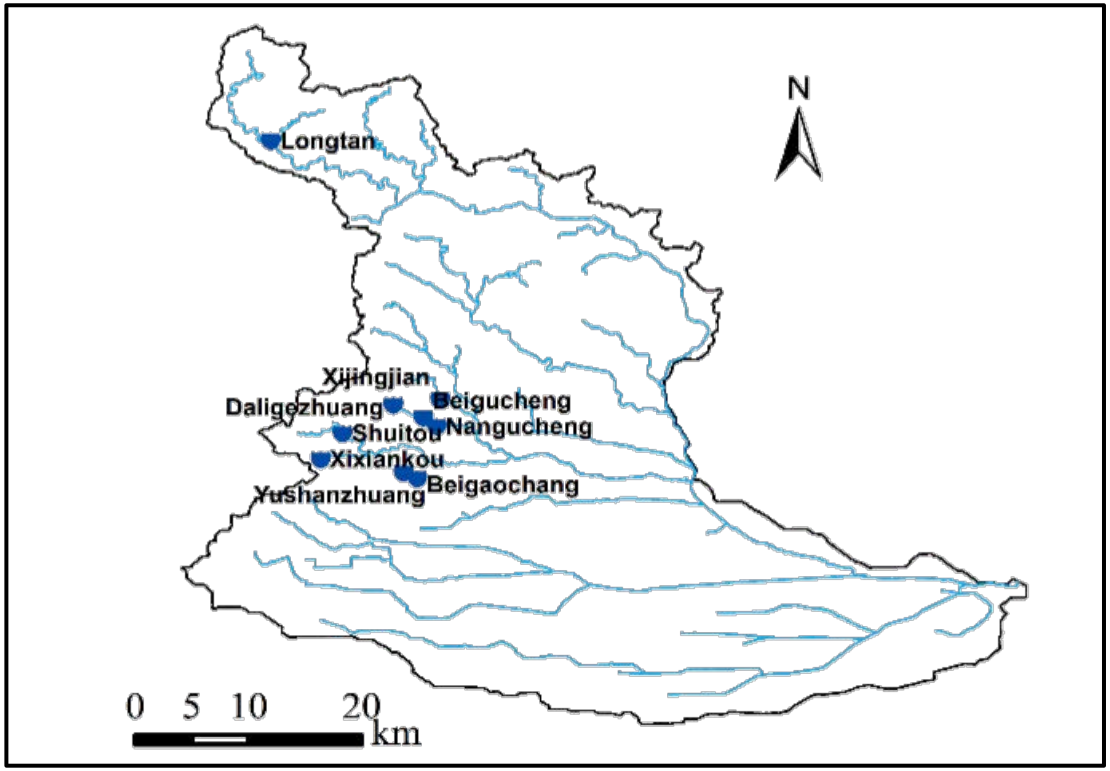

4. Modelling of runoff yield and concentration

Case study

Water body extraction of the Longtan Reservoir

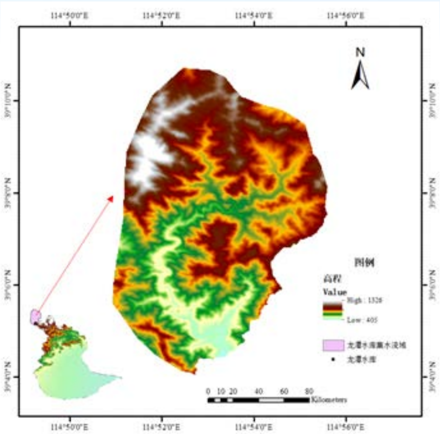

- Extract water information based on Landsat satellite using the iterative in-class variance maximization method
- Gain the latest reservoir water body images of 12 flood events

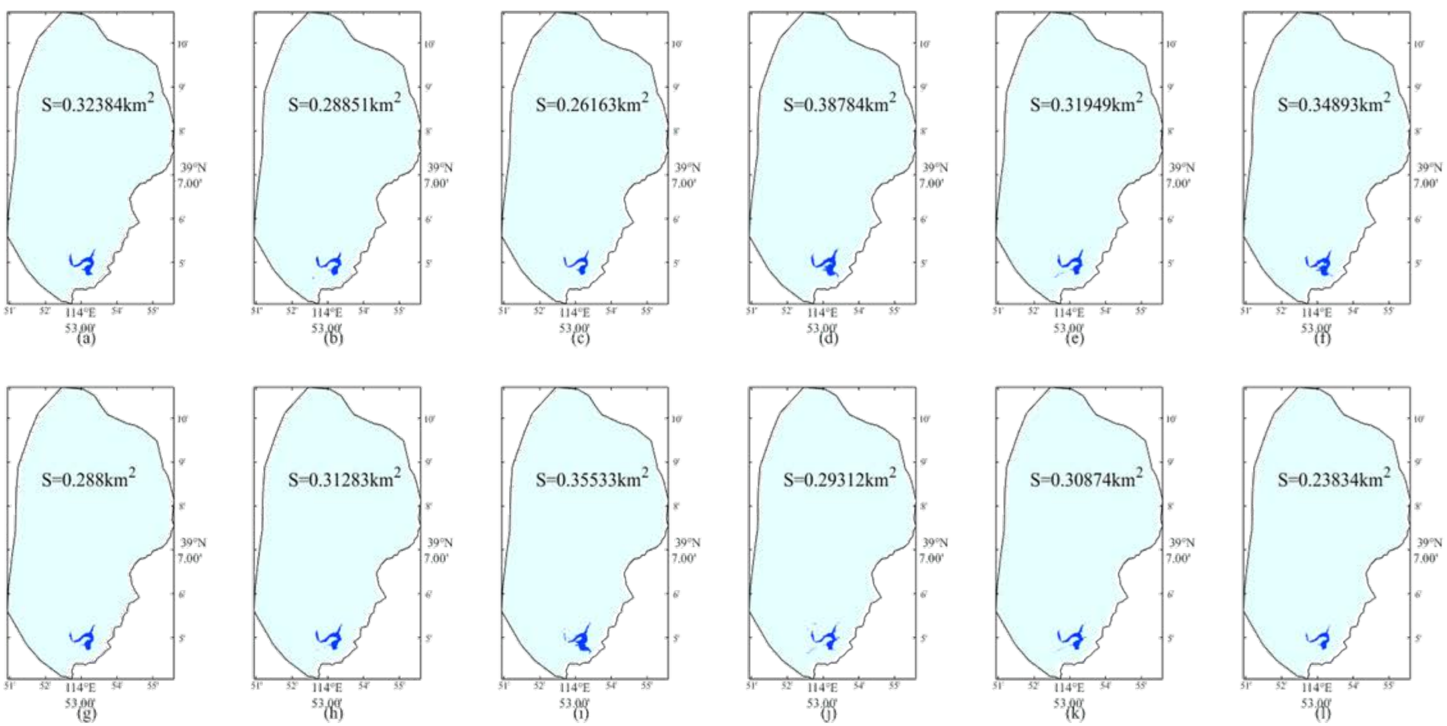

4. Modelling of runoff yield and concentration

Case study

Basic information of groundwater

- A total of 13 groundwater level monitoring stations in and around the watershed.
- Groundwater level across this watershed is high in the west and low in the east, since groundwater exploitation more happened in the eastern plain

Groundwater level monitoring stations

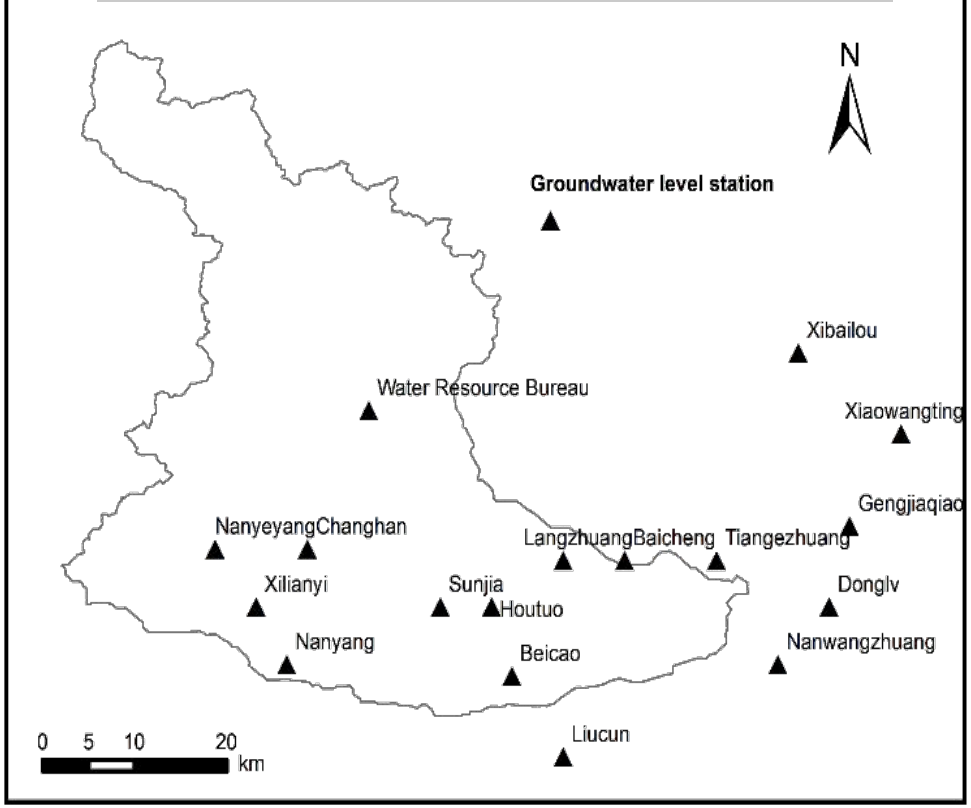

Altitude of groundwater level

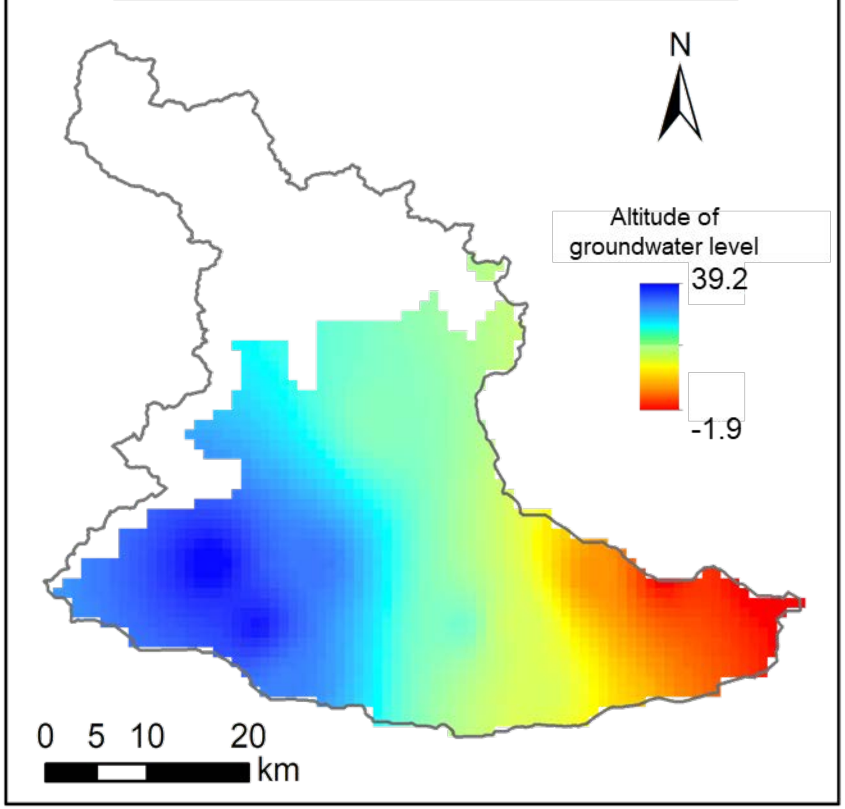

4. Modelling of runoff yield and concentration

Case study

Typical flood comparison

- Original simulation by gridded infiltration- and saturation-excess combination model (GIS, in orange), which is much larger than the observations (in blue)

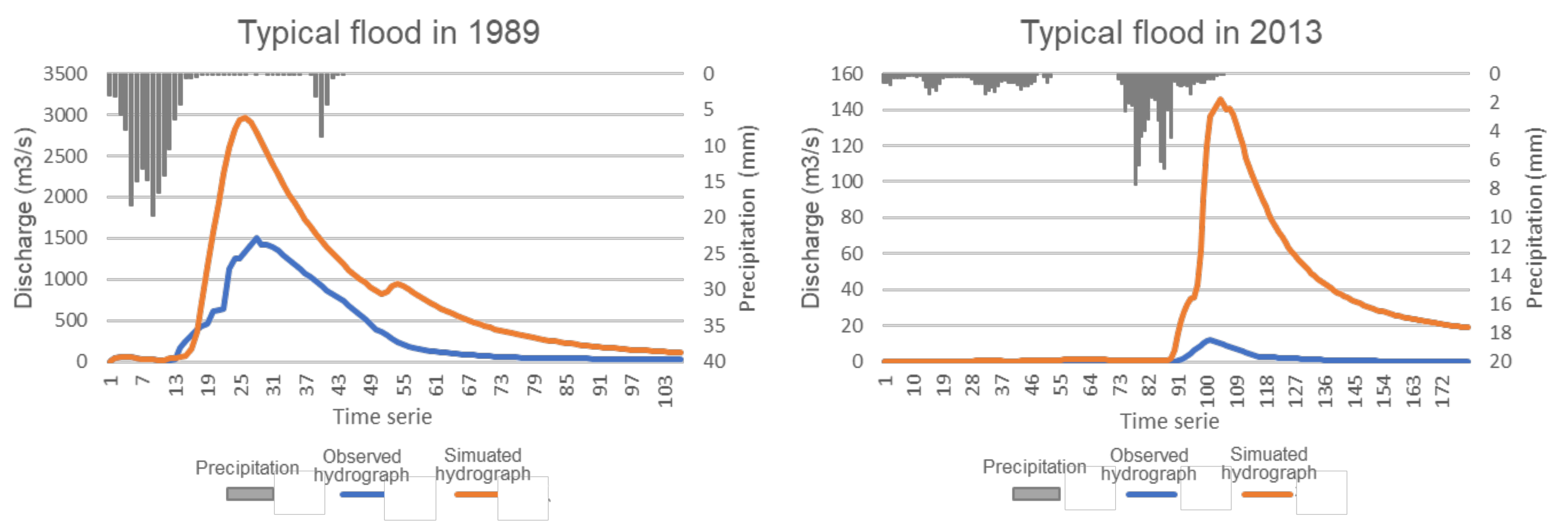

4. Modelling of runoff yield and concentration

Case study

Typical flood comparison

- Simulations by the GIS + aboveground regulation module (in yellow)
  - ✓ The simulated flood peak and flood volume are reduced to some extent
  - ✓ The model only considers the interception effect of water conservancy projects on surface runoff, and cannot fully reflect the impact of human activities

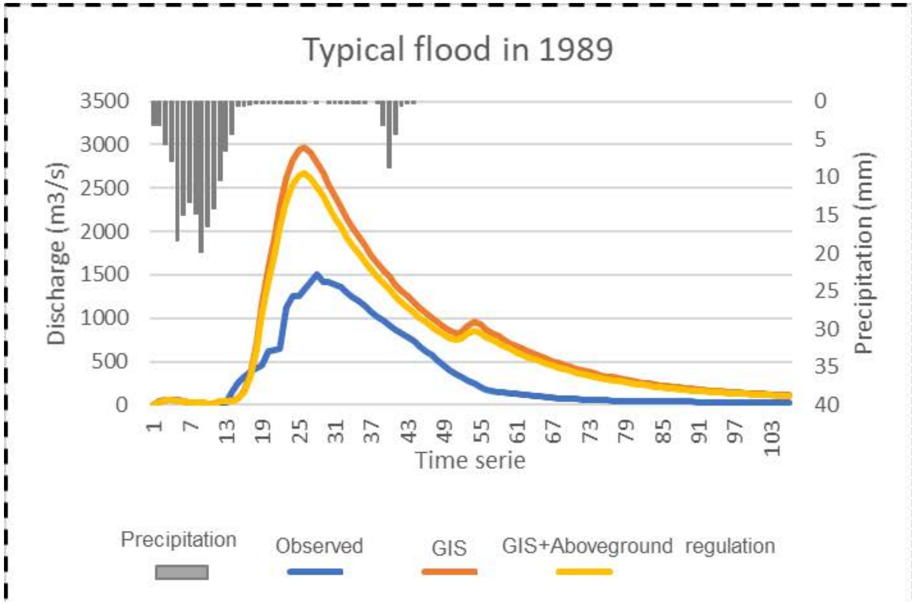

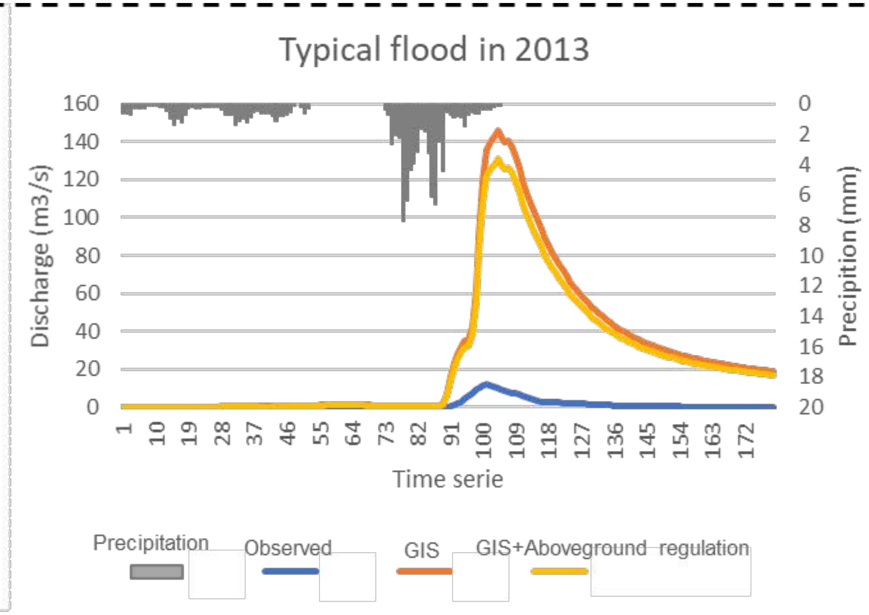

4. Modelling of runoff yield and concentration

Case study

Typical flood comparison

- GIS + underground regulation (in purple)

✓ The simulation accuracy of flood volume and peak is significantly improved, and the simulated flood process is basically consistent with the observed ones.

✓ The groundwater funnel plays a dominant role on the retention of runoff.

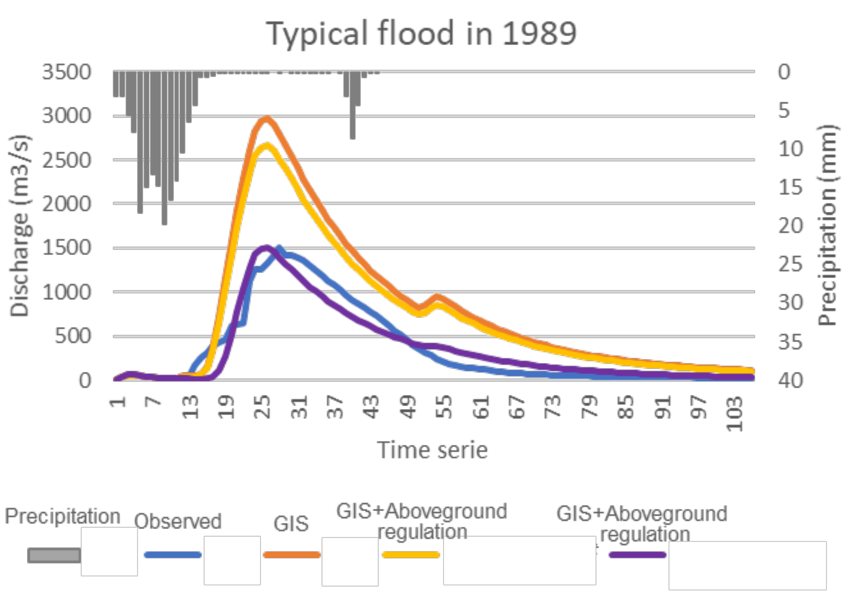

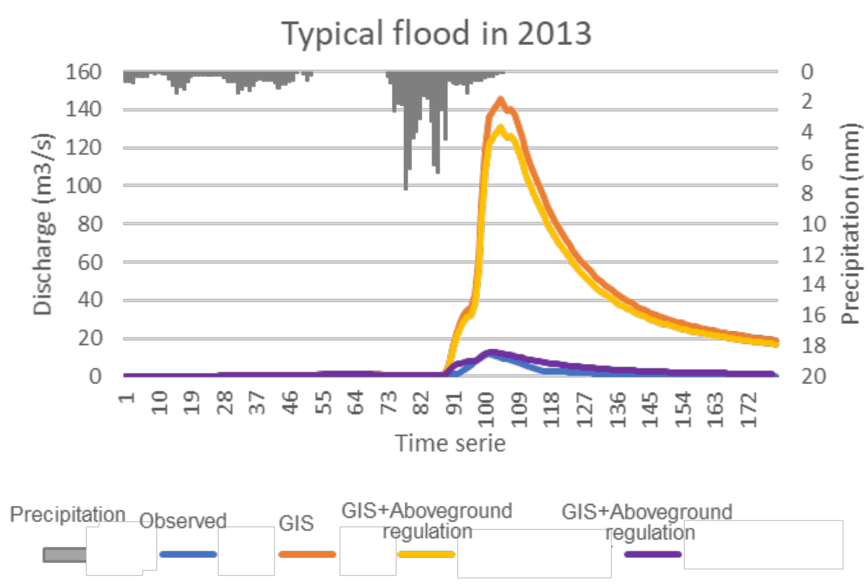

4. Modelling of runoff yield and concentration

Case study

Typical flood comparison

- GIS + dual regulation (in green)
  - ✓ The model shows similar performance to the GIS+underground storage model.
  - ✓ The model structure can more completely reflect the runoff generation mechanism under the influence of human activities.

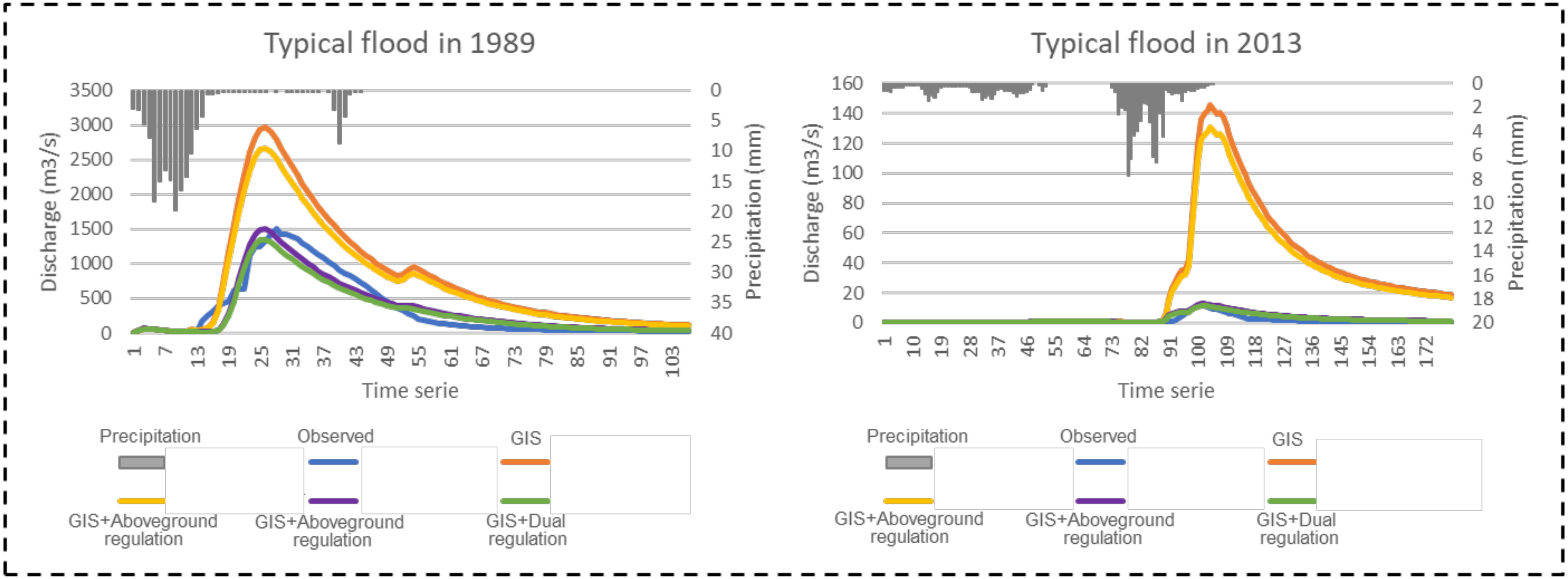

4. Modelling of runoff yield and concentration

Case study

Comparison of the qualification rate

Model	Flood volume	Flood peak	NSE>0.5
Emperical model	/	40%	/
Semi-distributed model			
XAJ model	75%	42%	17%
XC model	83%	50%	0
Distributed model			
GXAJ model	40%	45%	30%
GIS + aboveground regulation	40%	45%	30%
GIS + underground regulation	92%	75%	60%
GIS + dual regulation	92%	75%	60%

5. Conclusions

- Medium and small rivers are widely distributed in space, making their runoff yield modes dynamical and different with each other
- Human activities have imposed large impacts on watershed hydrological processes, which must be accounted in the model to achieve better flood forecasting accuracy
- Introducing the spatial combination of saturation-excess and infiltration-excess mechanisms, and the method to account for the aboveground and underground human regulation makes the model's predictive capability largely improved
- New technologies such as remote sensing, data fusion, and data assimilation are promising for enhancing the performance of process-based models

Thank you！